

DOI: 10.1002/marc.201800917

## Review

### pH-Responsive Polymer Nanoparticles for Drug Delivery

Nayeleh Deirram<sup>1</sup>, Changhe Zhang<sup>1</sup>, Sarah S. Kermaniyan<sup>1</sup>, Angus P. R. Johnston<sup>2</sup>,  
and Georgina K. Such<sup>1\*</sup>

---

<sup>1</sup> School of Chemistry, The University of Melbourne, Parkville, Victoria 3010, Australia

gsuch@unimelb.edu.au

<sup>2</sup> Monash Institute of Pharmaceutical Sciences, Monash University, Parkville, Victoria 3052, Australia

Stimuli-responsive nanoparticles have the potential to improve the delivery of therapeutics to a specific cell or region within the body. There are many stimuli that have shown potential for specific release of cargo, including variation of pH, redox potential, or the presence of enzymes. pH variation has generated significant interest for the synthesis of stimuli-responsive nanoparticles because nanoparticles are internalized into cells via vesicles that are acidified. Additionally, the tumor microenvironment is known to have a lower pH than the surrounding tissue. In this review, different strategies to design pH responsive nanoparticles are discussed, focusing on the use of charge-shifting polymers, acid labile linkages, and crosslinking.

## 1. Introduction

Polymer nanoparticles have the potential to improve the delivery of therapeutics due to their ability to protect fragile cargo until it reaches a target site. However, there are many biological roadblocks to achieving effective therapeutic delivery. These challenges include the ability to evade the immune system, target specific cells and tissue, and deliver cargo to specific intracellular regions. While there has been significant progress to overcome these barriers, there are still limited examples of polymer delivery systems used in the clinic<sup>[1]</sup>. To ensure delivery of a therapeutic cargo to the active site, one important strategy is the use of stimuli-responsive nanoparticles.<sup>[2,3,4]</sup> Such nanoparticles can be engineered to undergo changes in material properties when exposed to different biological stimuli. Many different stimuli have been used to design responsive nanoparticles including external stimuli e.g., temperature, light or biological stimuli such as pH or redox conditions.

This is the author manuscript accepted for publication and has undergone full peer review but has not been through the copyediting, typesetting, pagination and proofreading process, which may lead to differences between this version and the [Version of Record](#). Please cite this article as [doi: 10.1002/marc.201800917](#).

This article is protected by copyright. All rights reserved.

pH responsive nanoparticles have generated research interest due to the change in pH that occurs when nanoparticles are endocytosed into a cell. The pH drops from pH 7.4 in the blood-stream to approximately pH 6.5 in the early endosomal compartment, and below pH 5 in the lysosomal compartment.<sup>[5]</sup> There are also extracellular regions that have lower pH, including tumors which have been shown to be slightly acidic (~ pH 6.4-6.8).<sup>[5]</sup> pH responsive materials are also attractive as pH responsive functionality can be readily incorporated into a range of polymer structures to design a suite of pH responsive nanoparticles. Nanoparticles can be designed to respond to pH by changing surface chemistry, changing particle size or shape, disassembling or releasing cargo. This change in nanoparticle properties can be used to tune cell uptake and to control release of cargo. Thus, pH responsive nanoparticles offer a powerful strategy to engineer therapeutic delivery systems. Importantly, pH responsive nanoparticles have also shown the ability to disrupt the endosomal/lysosomal membrane<sup>[6]</sup>, thus insuring more efficient delivery to regions of the cell where the therapeutics are most active e.g., cytosol. In this review we will highlight three key strategies (Figure 1) to design pH responsive nanoparticles for therapeutic delivery. First, the use of charge shifting polymers, second, the use of acid labile linkages as pendant functionality. The third strategy involves the use of acid labile linkages to form crosslinked particles. Recent examples of how each of these strategies has been used to design interesting nanoparticle delivery systems will also be discussed.

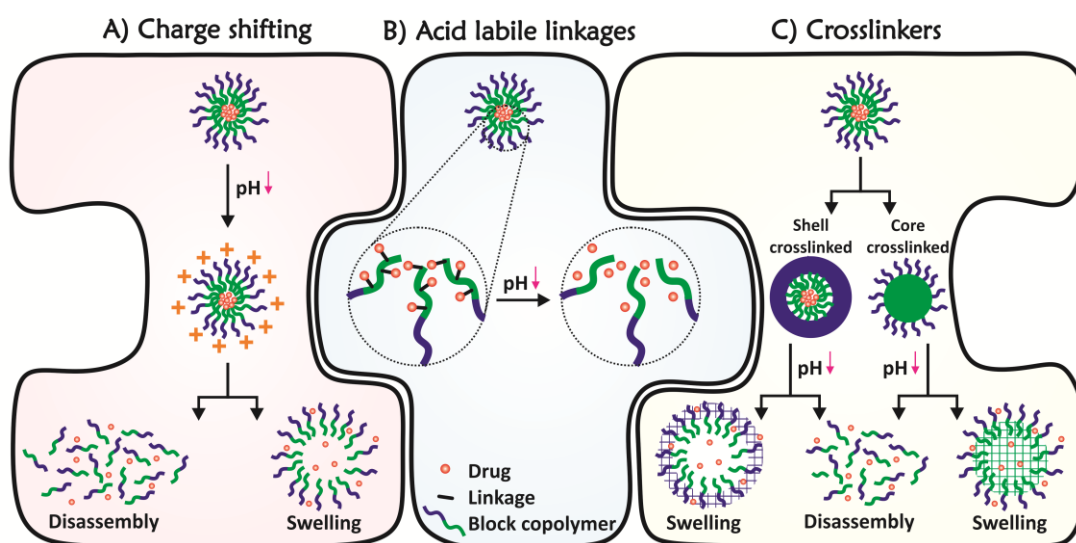


**Figure 1.** Strategies to engineer pH-responsive nanoparticles, including A) use of charge shifting polymers, B) acid labile linkages, or C) crosslinkers that can either combine charge shifting polymers with non-cleavable linkages to create swellable particles (covered in section 2) or acid-labile linkages which lead to pH responsive disassembly (Section 4).

## 2. pH-responsive charge shifting polymeric nanoparticles

A simple and effective strategy to design pH responsive materials is to use polymer building blocks, which change charge and/or hydrophilicity based on the pH of the environment. Changes in these properties can be used to induce variations in the nanoparticle structure such as rearrangement, swelling or disassembly. Charge shifting occurs based on the  $pK_a$  of the polymers.<sup>[7a]</sup> For drug delivery applications two types of polymers are commonly used, cationic polymers that change from hydrophobic to positively charged/hydrophilic when the pH is decreased or anionic polymers which go from negatively charged/hydrophilic to hydrophobic as pH is decreased.

### 2.1 Charge shifting from hydrophobic to hydrophilic with a decrease in pH

One of the most common types of charge shifting polymers are polymers which shift from hydrophobic to positively charged and hydrophilic when the pH decreases below their  $pK_a$ . These polymers contain amino groups, such as poly(2-(diisopropylamino)ethyl methacrylate) (PDPAEMA)<sup>[7b,8a]</sup>, poly(4-vinyl pyridine) (P4VP)<sup>[8b]</sup>, poly(histidine)<sup>[8c,9a]</sup> and poly( $\beta$ -amino ester).<sup>[7a]</sup> The main polymer structures discussed in this review are given in Table 1. The amino groups accept a proton and become hydrophilic when the environmental pH drops below their  $pK_a$ . To harness these polymers for the synthesis of drug delivery systems, one technique is to synthesize an amphiphilic block copolymer where the pH responsive block is hydrophobic at the pH of the bloodstream ( $\sim$  pH 7.4), thus forming self-assembled structures. When the pH is decreased, this block becomes hydrophilic, causing the polymer to be solubilized and thus the nanoparticle to disassemble. Liang et al. applied this strategy to design a one step nanoparticle delivery system including a model drug, PEG-doxorubicin (Dox) conjugate and a PDPAEMA homopolymer. The authors also incorporated an H4R4 peptide consisting of arginine (R) and histidine (H) groups. In acidic conditions PDPAEMA underwent a transition from hydrophobic to hydrophilic, causing disassembly of the nanoparticles and release of the Dox conjugate. They demonstrated release of the drug was pH dependent, at pH 7.4 only 10% of Dox release was observed however at pH 5.5 over 90% of the Dox was released after 36 hours. In addition, it was shown that loading the nanoparticle with H4R4 peptide caused a 30-fold increase in cell toxicity. The results of *in vitro* experiments with HeLa cells showed that the incorporation of H4R4 promoted localization of Dox into the nucleus.<sup>[9b]</sup>

Recently, we demonstrated a similar one step nanoparticle assembly using two pH-responsive polymer components, a homopolymer poly(2-diethylamino)ethyl methacrylate) (PDEAEMA) (38 kDa) and a diblock copolymer poly(2-diethylamino)ethyl methacrylate)-b-poly(ethylene glycol) (PDEAEMA-b-PEG) (16 kDa). We postulated that PDEAEMA forms the hydrophobic core of the nanoparticles while the PDEAEMA-b-PEG stabilizes the particle in physiological conditions. The mean size of these nanoparticles was approximately 150 nm. We used calcein (a small molecule) to investigate the endosomal escape induced by the nanoparticles. Calcein (green fluorescence) is trapped within the endosomal/lysosomal compartments of the cell if no particles are present (Figure 2a and 2c), however calcein is released into the cytosol when pH responsive nanoparticles are also

added and facilitate endosomal escape (Figure 2b, d).[10] Therefore, the calcein appears as diffuse fluorescence throughout the cell.

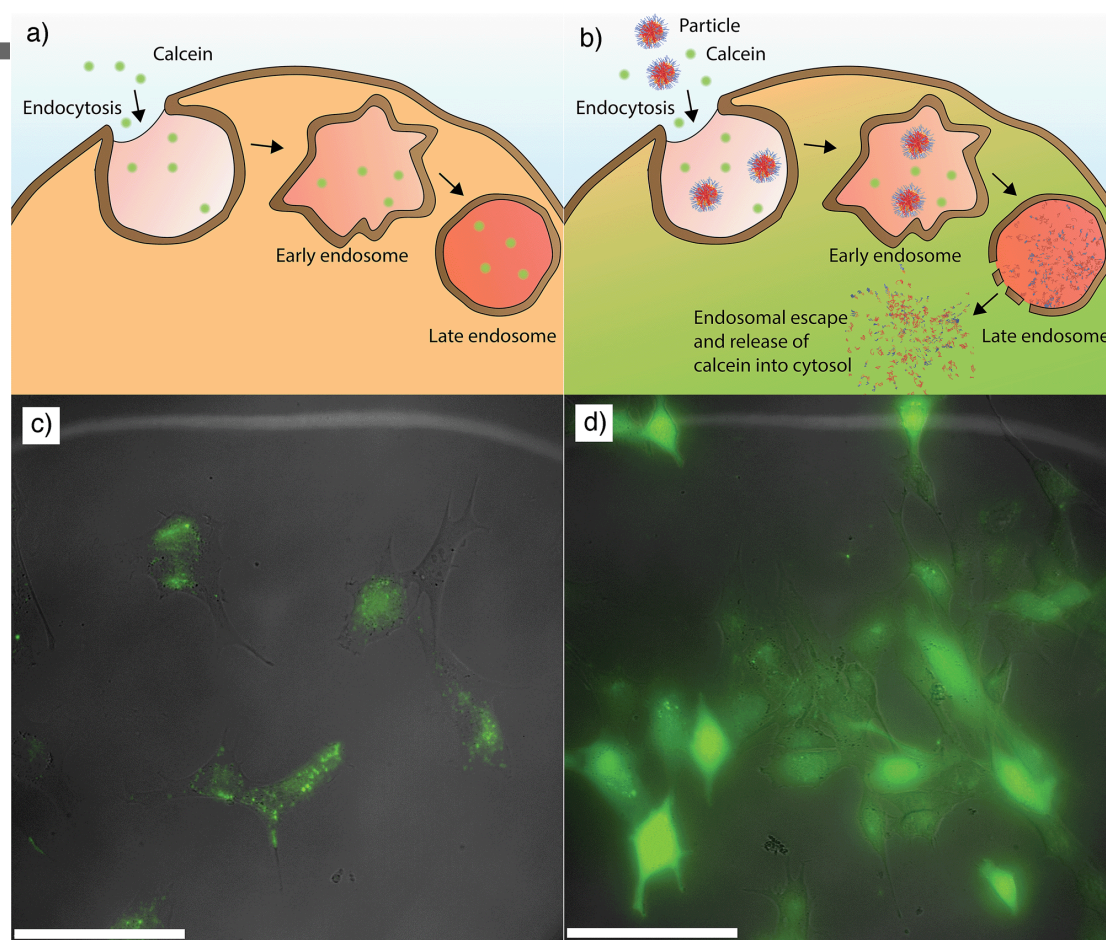


**Figure 2.** A) Schematic demonstrating the entrapment of calcein (green fluorescence) within endosomal/lysosomal compartments without nanoparticles (used as a control sample). B) Schematic showing the escape and release of calcein into the cytosol when combined with nanoparticles. C) Cellular microscopy images showing punctate distribution of calcein within the endosomal/lysosomal compartment indicating no endosomal escape. D) Cellular microscopy images showing  $\approx 30\%$  of cells with diffuse calcein throughout the cell. Adapted with permission.<sup>[10]</sup> Copyright 2015, Royal Society of Chemistry.

In later work, we designed a series of pH responsive nanoparticles combining poly (ethylene glycol)-b-poly(2-(diethylamino)ethyl methacrylate) (PEG-b-PDEAEMA) with random copolymers of 2-(diethylamino)ethyl methacrylate (DEAEMA) and 2-(diisopropylamino)ethyl methacrylate (DPAEMA). This work showed that by changing the molar ratio of DEAEMA and DPAEMA in the core polymer (1:0, 3:1, 1:1, 1:3 and 0:1) the disassembly of the nanoparticles could be tuned from pH 7.2 to pH 4.9 at 37 °C. It was also seen that the pH of disassembly affected the nanoparticle's capability to endosomal escape.[11]

Stayton and co-workers have used charge shifting polymers to design vaccine delivery systems.<sup>[12]</sup> In 2013, his group synthesized pH responsive nanoparticles of ~ 23 nm. The nanoparticles were formed by self-assembly of a charge shifting diblock copolymer. The hydrophilic block of the nanoparticle included 97% 2-(dimethylamino)ethyl methacrylate (DMAEMA) and 3% pyridyl disulfide ethyl methacrylate (PDSEMA). DEAEMA was used for complexation of oligonucleotide adjuvant (CpG ODN). PDSEMA was used for conjugation of ovalbumin (OVA) as a thiolated protein antigen through disulfide exchange. The pH responsive hydrophobic block was based on propyl acrylic acid (PPAA), DMAEMA and butyl methacrylate (BMA). When the nanoparticles were exposed to the low pH of the endosome, the nanoparticles disassembled, interacted with the endosomal membrane and released their antigen and adjuvant cargo. This study reported that vaccination of mice with the OVA-conjugated nanoparticles showed significantly higher CD8<sup>+</sup> T cell response (0.5% IFN- $\gamma$ <sup>+</sup> of CD8<sup>+</sup>) compared to mice vaccinated with free OVA. They also reported that the immunization with OVA-conjugate nanoparticles which included the CpG ODN caused an increased CD8<sup>+</sup> T cell response (3.4% IFN- $\gamma$ <sup>+</sup> of CD8<sup>+</sup>) 7-, 18-, and 8-fold relative to immunization with conjugates, OVA administered with free CpG, or a formulation containing free OVA and CpG complexed to micelles, respectively.<sup>[12]</sup> Stayton and co-workers have also investigated the use of different hydrophilic components for particle design<sup>[13]</sup> and the use of different architectures.<sup>[14]</sup> In the work using different architectures they showed that nanoparticles with more globular structures e.g., hyperbranched, enhanced the ability to achieve a strong immune response.

Similar nanoparticles were also used to deliver a pro-apoptotic peptide.<sup>[15]</sup> Stayton and co-workers used a diblock copolymer to make pH responsive nanoparticles with a therapeutic peptide loaded through an enzyme cleavable linkage. The hydrophilic segment of the polymer included poly(ethylene glycol) methacrylate (PEGMA) for biological stability, and the methacrylamido-peptide macromonomer as the therapeutic component.<sup>[15]</sup> The pH responsive block was based on pH responsive DEAEMA and butyl methacrylate (BMA). It was shown that this particle could disassemble when the pH was decreased and had potential to cause endosomal escape through membrane interaction. Apoptosis markers increased 8-fold with the delivery of a pro-apoptotic peptide compared to the carriers loaded with a scrambled sequence.

Gao and co-workers have designed an elegant block copolymer system using poly(ethylene oxide) (PEO) as the hydrophilic component and a range of tertiary amine monomers as hydrophobic (PR) blocks to synthesis pH-activatable micellar (pHAM) systems.<sup>[16]</sup> In their early work they reported the pH dissociation of the micelles could be tuned by using different combinations of ionizable PR blocks. They prepared two types of functionalized PR block, (i) a series of linear dialkyl moieties with different chain lengths from methyl to butyl groups and (ii) a cyclic series where the ring size was varied from five- to seven-membered rings. The authors then conjugated the pH insensitive dye tetramethyl rhodamine (TMR) to investigate the pH-dependent response of the respective micelles (PR block). The PR group is hydrophobic when the pH is higher than the  $pK_a$  of the responsive micelle system, resulting in particle self-assembly and quenching of fluorescence signal through photoinduced electron transfer and homo-FRET. However, when the pH is lower than the  $pK_a$ , the PR group become protonated causing disassembly of the micelle and significantly increasing the

fluorescence. Using this technique the authors could determine the internalization of their particles into endosomal/lysosomal cell compartments by following an increase in fluorescence intensity.<sup>[16]</sup>

Gao and co-workers also reported the design of pH responsive micelleplexes for the delivery of siRNA.<sup>[17]</sup> The micelles were formed by self-assembly of PDMAEMA-*b*-PDPAEMA diblock copolymers. At the pH of the blood stream (pH 7.4), the PDPAEMA block self-assembled to form hydrophobic cores allowing the encapsulation of a hydrophobic drug (Amphotericin B). PDMAEMA acted as the positive charged shell that allows for siRNA complexation. It was shown that the complex of PDMAEMA-*b*-PDPAEMA/siRNA dissociates at low pH and the hydrophobic Amphotericin B drug is released.<sup>[17]</sup> It was also observed that the amphotericin B enhanced the delivery of the siRNA by improving endosomal escape.

In 2017, Battaglia and co-workers used charge shifting building blocks to design pH responsive nanoparticles to enhance delivery of Dox (a cancer drug). They used gold nanoparticles (AuNPs) as a core for anchoring triblock copolymers of poly(oligo(ethylene glycol)methyl ether methacrylate) PEOGMA, PDPAEMA and poly(2- (methacryloyloxy)ethyl phosphorylcholine) PMPC (PEOGMA-*b*-PDPAEMA-*b*-PMPC). The synthesis of the triblock copolymer was performed by atom transfer radical polymerization (ATRP) from a disulfide initiator. In this system PDPAEMA acts as pH responsive monomer for encapsulating the hydrophobic drug Dox. Drug release occurred at pH 6 when the polymer became charged. The PMPC outer corona was designed to increase the colloidal stability in biological media. The authors treated MCF-7 breast cancer cells with Dox-loaded nanocarriers to investigate the efficiency of cell killing compared to nanocarriers without Dox. The cell viability results showed the Dox-loaded nanoparticles had significantly higher toxicity than the free Dox (0.2 cell viability compared to 0.8 for free Dox, normalized to untreated cells (1.0)).<sup>[18]</sup>

Recently, Gao and co-workers designed biosensors using a disulfide-based, redox-activatable fluorescence sensor (qRAS). They synthesized the sensor by conjugating a pH insensitive fluorescence donor (TMR) and acceptor (Cy5) onto the same cystine, one of these linkages was through a disulfide bond. In the off state, the donor fluorescence is quenched, so just one emission peak is reported. However, when the disulfide moiety is cleaved by glutathione (GSH) in the cell cytosol, the donor and acceptor are no longer in close proximity and thus the fluorescence of the donor can be observed (Figure 3). The authors showed that the fluorescence of the donor increased by 70-fold with the addition of 5 mM tris(2-carboxyethyl)phosphine TCEP. They also used OVA as a model protein labeled with qRAS. They showed that addition of reducing agent significantly increased the fluorescence intensity (30-fold).<sup>[19]</sup> This sensor was used to investigate the cytosolic delivery of a library of pH responsive nanoparticles to determine which nanoparticle exhibited the best endosomal escape.<sup>[19, 20]</sup> Results showed the PC7A NPs had a highest fluorescence change of approximately 22 %.

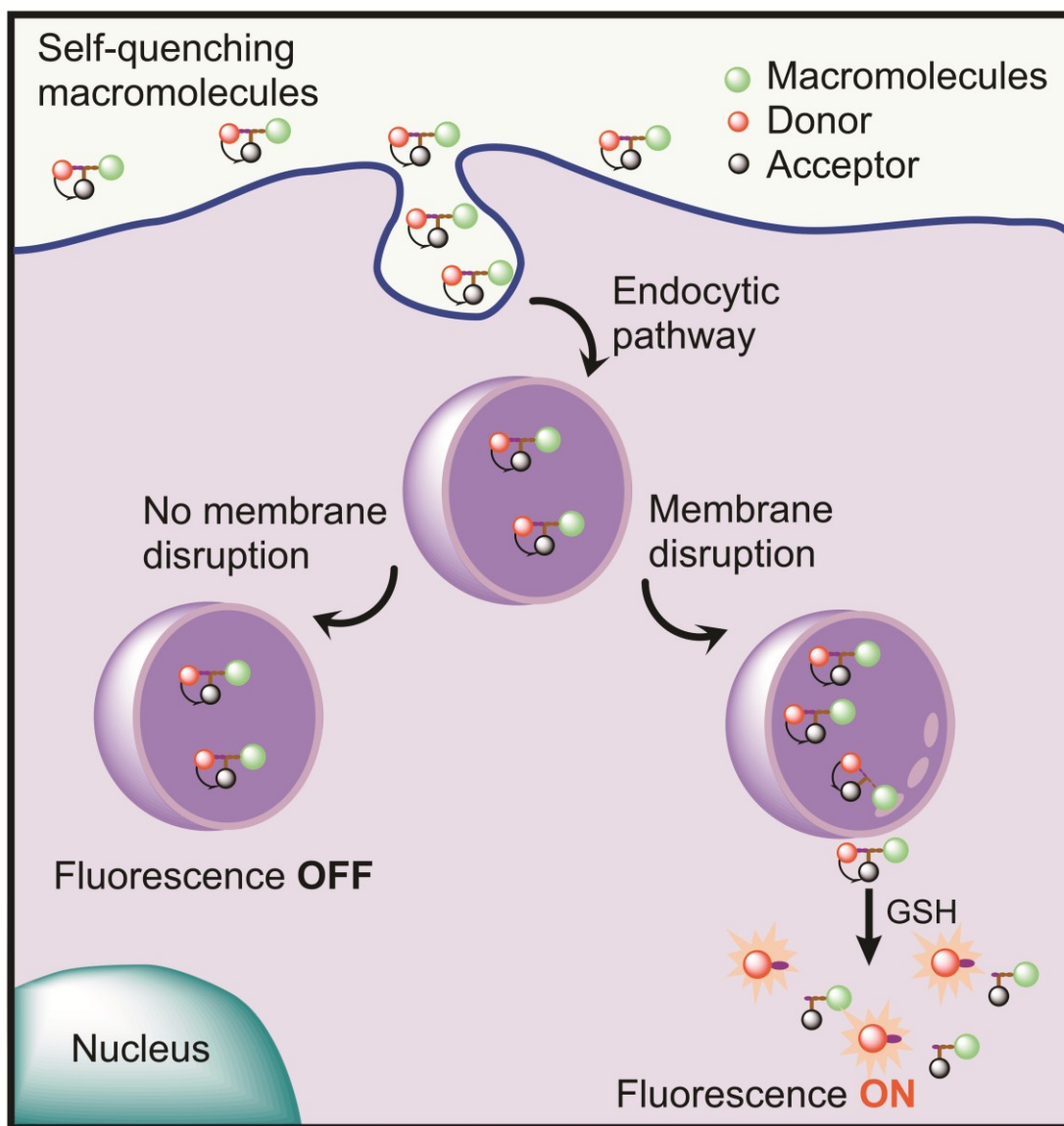


**Figure 3.** Design of biosensors by using disulfide-based, redox-activatable fluorescence sensor (qRAS). The fluorescence of the donor molecules is off when the two fluorophores are in close proximity due to FRET, which occurs in the extracellular region and also in the endosome/lysosome. However, after the sensor escapes into the cytosol the disulfide bond can cleave, thus the two fluorophores are no longer close together and two signals can be observed. Adapted with permission.<sup>[19]</sup> Copyright 2017, Wiley-VCH.

In later work, Gao and co-workers used a library of ultra pH sensitive (UPS) NPs containing tertiary amine with linear or cyclic side chains and then loaded OVA as a model antigen (Figure 4a). To investigate antigen presentation, mice were vaccinated with the different OVA loaded particles. It was found the PC7A NPs had the highest cytotoxic T lymphocyte (CTL) mediated killing (Figure 4b).<sup>[20]</sup> Interestingly, they also used these particles to load a range of therapeutic antigens and tested the ability of the antigen loaded nanoparticles to kill their respective tumors. In the human papilloma virus E6/7 TC1 tumors, 100 % of the animals survived for over 100 days and 90 % were tumor free.

Multidrug resistance (MDR) is a significant problem for therapeutic delivery, as it results in chemotherapeutic drugs becoming less effective over time. This resistance is caused either by less efficient uptake of the drug or more efficient efflux of the drug from the cell. Nanoparticles have shown potential to achieve more effective delivery into the cell and thus can help with this issue. Yu et al., looked at MDR by designing of set of nanoparticles containing PDPAEMA which allowed delivery of small interfering RNA (siRNA),<sup>[21]</sup> photosensitizer,<sup>[22]</sup> and anticancer drug<sup>[23]</sup>. Due to the protonation of PDPAEMA in the core at low pH, dissociation of the nanoparticles occurred in the early endosome, leading to release of drugs. In 2015, these authors reported pH and NIR-light responsive hybrid micelles based on a pluronic copolymer P123 conjugated Dox prodrug (P-Dox) and cypate-conjugated poly(ethylene glycol)-*b*-PDEAEMA (PEG-*b*-PDPAEMA) diblock copolymer (P-cypate), referred to as P-Dox/P-cypate. In the bloodstream (pH 7.4), the P-Dox/P-cypate micelles maintained their structure with nanoparticle size of ~ 30 nm however, in acidic regions when the pH was around 6.2, the micelles quickly disassembled leading to release of the P-Dox payload. The authors reported a combination of pH responsive and NIR laser irradiation showed significantly improved therapeutic efficacy of P-Dox/Pcypate micelles for treatment of Dox-resistant MCF-7/ADR breast cancer.<sup>[24]</sup>

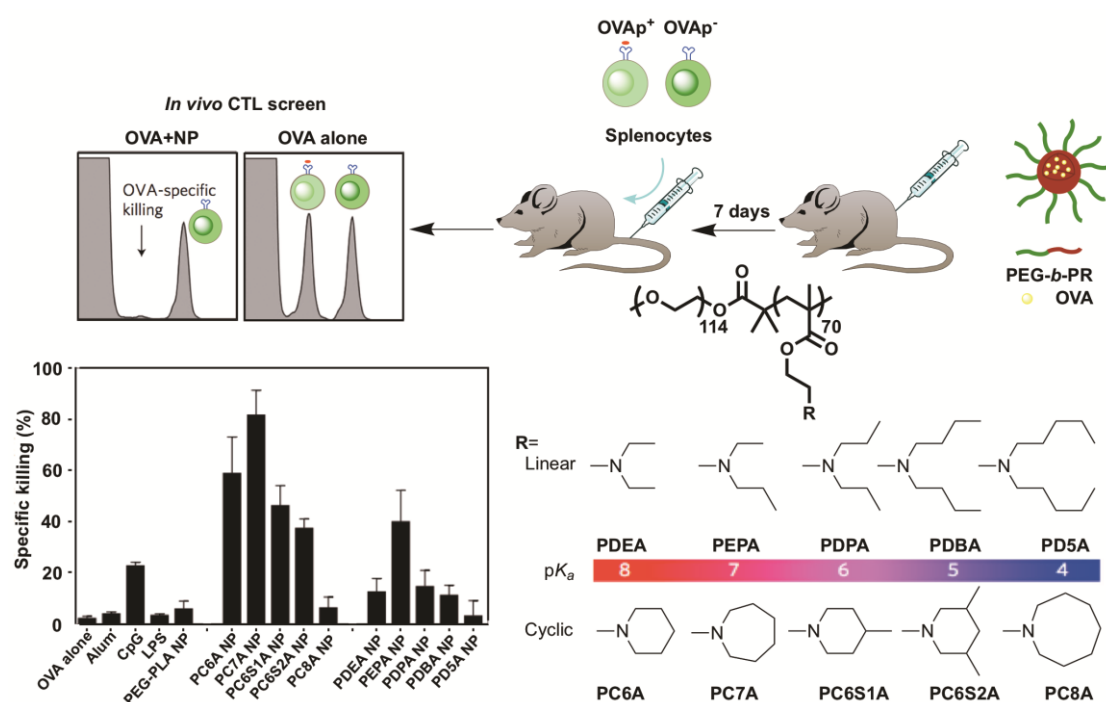


**Figure 4.** A) Schematic illustrating a mouse being vaccinated with a library of ultra pH-sensitive (UPS) OVA-NPs with different pK<sub>a</sub> and also R groups, and the comparison of cytotoxic T lymphocyte (CTL) production for different nanoparticles groups. B) Results of in vivo CTL assay for different formulations. Adapted with permission.<sup>[20]</sup> Copyright 2017, Macmillan Publishers Limited.

Another challenge for delivery of cancer therapeutics is tumor penetration. Recently, Jun Wang and his group developed ultra-pH sensitive cluster nanobombs (SCNs) with the ability to change particle size with variation in pH. The platinum (Pt)-prodrug conjugated SCNs (SCNs/Pt) were self-assembled from a super structure of poly(ethylene glycol)-*b*-poly(2-azepane ethyl methacrylate)-modified PAMAM dendrimers (PEG-*b*-PAEMA-PAMAM/Pt). The PAMAM act as a pH responsive monomer in this system. At pH 7.4 the size of super structure was around 80 nm in diameter. The PAMAM block was hydrophobic and directed the assembly of PEG-*b*-PAEMA-PAMAM/Pt into SCNs/Pt. However, in acidic tumor microenvironments (pH ~6.5–7.0), PAMAM becomes hydrophilic, leading to rapid decomposition of SCNs/Pt into small nanoparticles (< 10 nm). This approach was shown to facilitate more effective tumor penetration.<sup>[25]</sup>

Charge shifting polymers can also be used to synthesise particles that swell in response to a change in pH by incorporating crosslinkers into the particle<sup>[26]</sup>. One important study involved the synthesis of PDEAEMA-core/(2-aminoethyl methacrylate) PAEMA-shell nanoparticles by emulsion polymerization<sup>[24]</sup>. First, DEAEMA was polymerized with poly(ethylene glycol) dimethacrylate (PEGDMA) as a crosslinker to form the pH-sensitive core of the particles. Second, 2-aminoethyl methacrylate (AEMA) was added to the stirred latex suspension to polymerize a hydrophilic shell layer.<sup>[27]</sup> The size of the nanoparticles was tested using dynamic light scattering (DLS). At extracellular/cytosolic pH (7.4), the tertiary amines of DEAEMA in the particle cores are largely uncharged, and thus the particles were collapsed with a particle size of ~ 250 nm. However, at endolysosomal pH 5.0, the tertiary amines in the core ionize, which leads to the particle swelling to ~ 550 nm.<sup>[27]</sup>

## **2.2 Charge shifting from hydrophilic to hydrophobic with a decrease in pH**

In contrast to polymers synthesized from basic monomers, by using polymers synthesized from acid monomers, such as poly(methacrylic acid) (PMAA),<sup>[28,29,30]</sup> poly(aspartic acid) (PAsp),<sup>[30]</sup> and sulfonamide-based polymers<sup>[31]</sup>, it is possible to engineer nanoparticle delivery systems that become more hydrophobic in response to a decrease in pH.<sup>[32,33]</sup> Bae and co-workers developed negatively charged sulphonamide-based oligomers (OSAs) that shift from hydrophilic to hydrophobic with a drop in pH and also have proton buffering capacity. The authors tuned the  $pK_a$  of the OSA from pH 3–11 based on the choice of side chain such as sulfamethizole (OSMT), sulfadimethoxine (OSDM), sulfadiazine (OSDZ) and sulfamerazine (OSMZ).<sup>[34]</sup> They investigated the proton buffering capacity and pH based solubility transition of OSAs. OSMT and OSDZ had broad proton buffering in the pH range between 5–6.4 and 5.7–7.3 respectively, however, the proton buffering of OSDM and OSMZ occurred at pH 6.5 and 7.3 respectively. They used different cell lines such as (HEK293, HepG2, and RINm5F cells) to investigate the nucleic acid delivery *in vitro*. OSA-polyplexes were designed by

combining the sulfonamide polymer with DNA and then complexing with poly(L-lysine) (PLL). They found that OSDZ polyplexes and OSMZ polyplexes has a maximum transfection compared to PLL/DNA controls (approximately 12-fold and 55-fold respectively) against HEK293 and RINm5F cells.<sup>[34]</sup>

Functional groups that become hydrophobic when the pH is decreased can enhance destabilization of the endosomal membrane and thus facilitate endosomal escape. An important example is the use of poly(propyl acrylic acid) (PPAA). Stayton et al<sup>[35,36a]</sup> reported that PPAA dramatically increased *in vitro* transfection efficiencies of a lipoplex formulation in mouse fibroblast cells (NIH3T3). In addition, they reported that when they used poly(acrylic acid) (PAA) instead of PPAA, the results were not as effective. The authors demonstrated that the increase in transfection by PPAA occurs due to the repeating propyl groups in the backbone of PPAA.<sup>[36b]</sup>

Charge shifting materials have significant potential for drug delivery applications as they can be engineered to respond in a specific pH range, while maintaining good stability in the blood stream. In addition, their response is typically fast, as it does not require cleavage of bonds to facilitate change in particle structure. These materials have also shown potential to facilitate endosomal escape, a key roadblock for delivery of biological cargo. However, there is still significant work needed to understand how these systems interact with the biological environment e.g., the mechanisms of endosomal escape and the long term stability (aggregation and hydrolysis) of the nanoparticles in the body. It is important these fundamental studies be carried out alongside more applied work so we can understand how to design better pH responsive nanoparticles

### 3. pH responsive polymers with H<sup>+</sup> labile linkages

To design effective drug carriers the cargo needs to be loaded into nanoparticles and released at a specific location within the cell. To harness the inherent pH drop that occurs when nanoparticles are internalized, one strategy is to design nanoparticles containing covalent pH-responsive linkages that are stable at neutral pH but labile at acidic pH. While physical loading within a nanoparticle is possible, conjugation of drugs to polymeric materials allows better control over distribution and degradation, i.e., the drug-polymer conjugates are stable in body fluids but degrade specifically in cancer cells.<sup>[37]</sup> The following section discusses the synthesis of pH-responsive polymeric nanoparticles with acid labile linkages. The pH-responsive linkages that will be discussed include hydrazone, imine, acetal/ketal, *ortho* ester, *cis*-aconityl group and  $\beta$ -thiopropionate moieties.<sup>[37a]</sup> The general structures and the corresponding hydrolyzed products are summarized in Figure 5.

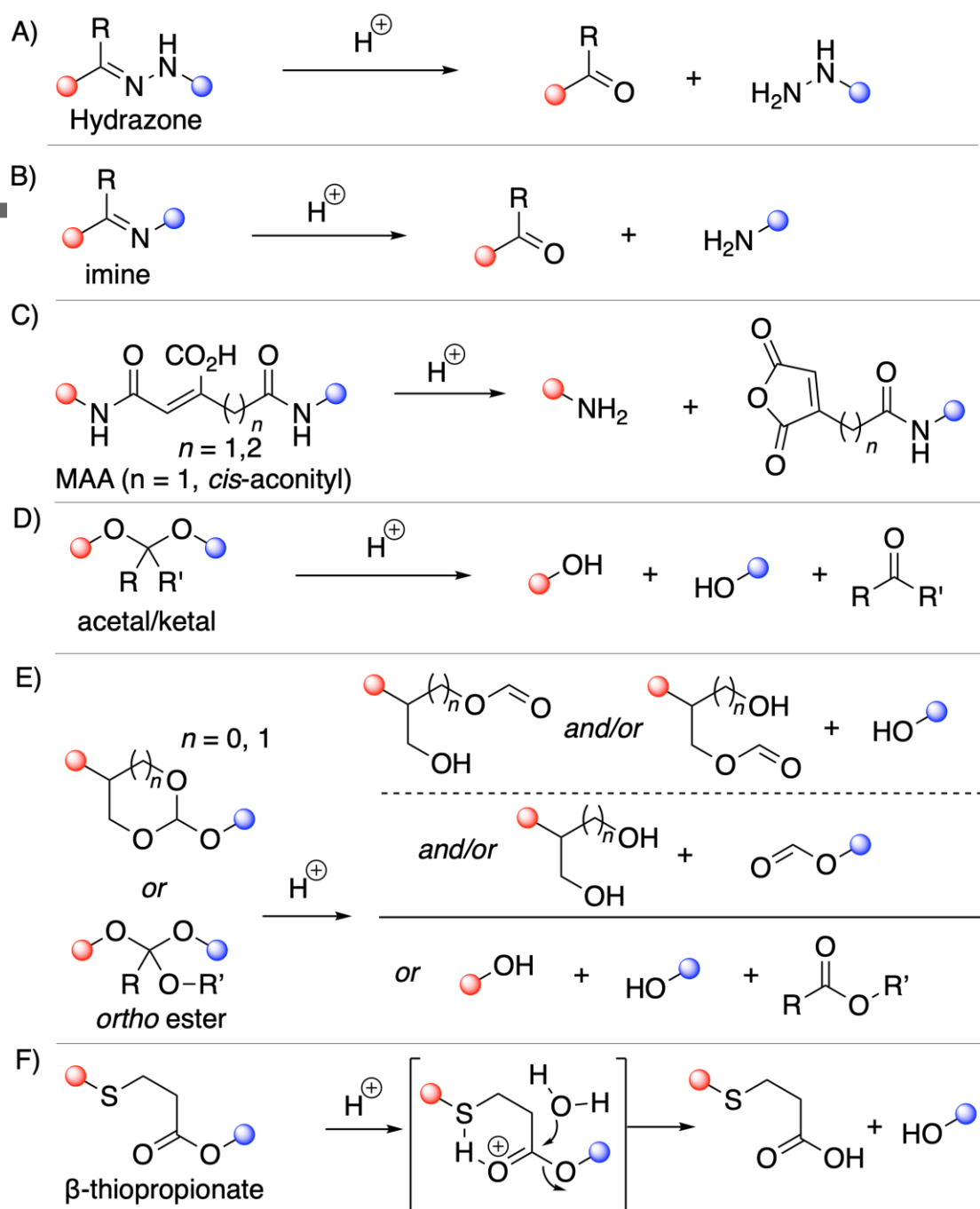


**Figure 5.** pH-Responsive linkages and the corresponding hydrolyzed products. A) Hydrazone linkages with ketone/aldehyde and hydrazide as the hydrolyzed products; B) imine linkages with aldehyde (ketone) and amine as the hydrolyzed products; C) maleic acid amide (MAA) linkages with amine and maleic anhydride as the hydrolyzed products (when  $n = 1$ , they are commonly denoted as *cis*-aconityl linkages); D) acetal/ketal linkages with two alcohols and aldehyde/ketone as the hydrolyzed products; E) *ortho* ester linkages with alcohols and formate or ester as the hydrolyzed products depending on the structures of the *ortho* ester structures; F)  $\beta$ -thiopropionate linkages with  $\beta$ -thiopropionic acid and alcohol as the hydrolyzed products.

### 3.1. Hydrazone linkages

The hydrazone linkage (A, Figure 5) is one of the most commonly used linkages in pH responsive drug delivery systems. At pH 7.4, the hydrazone bond is relatively stable and hydrolyzes very slowly, while in endosomal/lysosomal compartments (pH 5~6), the rate of hydrolysis is increased.<sup>[38]</sup> Dox and poly(*N*-(2-hydroxypropyl)methacrylamide) (HPMA), a hydrophilic biocompatible polymer, have been widely used as hydrazone linked polymer-drug conjugates and in nanoparticle delivery systems.<sup>[39]</sup> Etrych and co-workers were among the first to use the H<sup>+</sup> labile hydrazone linkages, enabling controlled drug release in mild acidic environments (pH 5.0).<sup>[40]</sup> Specific advantages include high drug loading, straight-forward preparation of polymer precursors, specific drug release and as a result, higher antitumor activity.<sup>[39b]</sup>

Hydrazone chemistry can also be used to engineer pH responsive nanoparticles. Zhang and co-workers reported antitumor nanoparticles of polymer-cisplatin conjugates linked by hydrazone bonds.<sup>[41]</sup> Modification of poly(ethylene glycol)-*b*-poly(L-lactide) (PEG-*b*-PLA), with hydrazine hydrate gave the polymer PEG-PLA-NH-NH<sub>2</sub> carrying hydrazide end groups which reacted with the ketone groups in the Pt(IV) prodrug to give the polymer-drug conjugate Bis(PEG-PLA)-Pt(IV). Nanoparticles (NPs) were prepared via the precipitation method. It was shown that drug release was tunable with pH, 50% release was observed after 4 h, 6 h and 22 h for pH 5.0, 6.0 and 7.4, respectively.

In 2012, Caruso and co-workers used the hydrazone bond to achieve pH-dependent drug release from polymeric particles (Figure 6).<sup>[42]</sup> The doxorubicin conjugated polymer was synthesized via thiol-maleimide click chemistry of thiolated poly(methacrylic acid) (PMA<sub>SH</sub>) and maleimide-functionalized doxorubicin (MAL-Dox) derivative with a hydrazone bond. The particles were prepared via mesoporous silica-templated assembly. At endosomal/lysosomal pH the hydrazone bond was cleaved causing the Dox to be released. Approximately 80% release occurred at pH 5.5 in 24 h, while there was limited release at pH 7.2 (~20%). Interestingly, the IC<sub>50</sub> of the nanoparticles (~28.5 nM) was lower than the free Dox formulation (~62 nM).

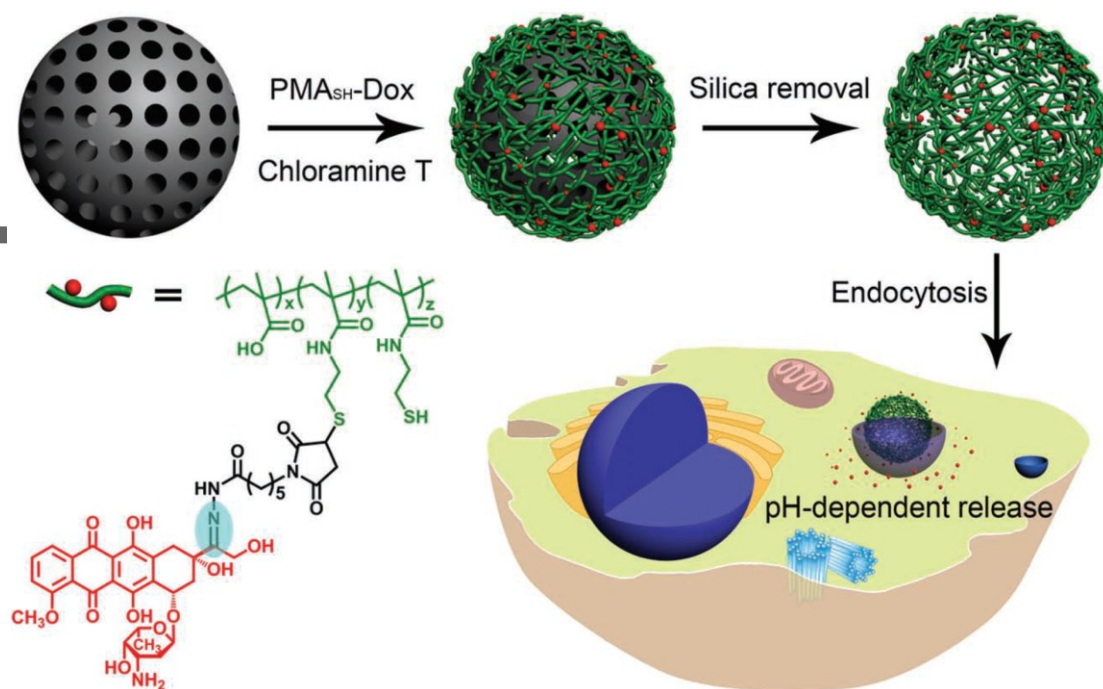


**Figure 6.** Schematic illustrating formation of the thiol modified poly(methacrylic acid) (PMA<sub>SH</sub>) nanoparticle with Dox loaded through a hydrazone bond and then specific drug release within the cell. Reproduced with permission.<sup>[42]</sup> Copyright 2012, Wiley-VCH.

Zhang and co-workers evaluated the effect of cationic side-chains on intracellular uptake and cytotoxicity of polymer-Dox nanoparticles.<sup>[43]</sup> The polymers were synthesized via Michael addition combining a molar ratio of 7 : 39 : 4 of PDA [2-(pyridylthio)-ethylamine], primary amine with a cationic side chain and poly(ethylene glycol) (PEG). Dox was conjugated to the polymer by reacting the PDA monomer with maleimide carrying a hydrazide, which then reacted with the Dox. Three different cationic side-chains, arginine methyl ester, histamine and tertiary amine, were investigated. It was found that tuning the cationic group lead to changes in cell viability. The IC<sub>50</sub> was ~173 ng/mL for histamine, arginine methyl ester was ~193 ng/mL and the tertiary amine was ~359 ng/mL. The different nanoparticles also showed different cell localization behavior.

Hydrazone linkages have also been used to conjugate drugs onto hyperbranched nanoparticles. Thurecht and co-workers have developed hyperbranched polymers carrying a peptide aptamer to target and chemosensitize Hsp70 (heat shock protein 70). The particles also contained Dox as the model antitumor drug and Cy5 (cyanine-5) as an imaging agent.<sup>[44]</sup> Dox was linked via pH-responsive hydrazone linkages, and 80 % release was observed at pH 5.0 compared to less than 10 % at pH 7.4 after 48 h. PAMAM dendrimers have also been designed with hydrazone linkages to conjugate Dox.<sup>[45]</sup> This work showed that the drugs conjugated via hydrazone linkages improved killing of cells over amide conjugated drug. It also demonstrated cell viability was comparable to free drug when using sensitive or resistant cells. Luo and co-workers developed a drug delivery vehicle based on mPEGylated peptide dendrons with Dox conjugated through a hydrazone bond.<sup>[46]</sup> PEGylation was crucial to increase the drug loading, blood circulation time and accumulation in tumor tissues. The drug Dox was released in acidic media (80% at pH 5.0 vs. 20% at pH 7.4 after 54 h) due to the hydrazone linkers. While the IC<sub>50</sub> of the nanoparticles was higher than free Dox *in vitro*, *in vivo* a

decrease in tumor size was observed when using the nanoparticle formulation. Histological analysis on a range of mice organs (e.g., heart, lung, spleen) showed no abnormal pathology, suggesting limited toxic side effects from the dendrimers.

A range of backbones have been combined with hydrazone linkages and Dox to design nanoparticles including poly(hexyl methacrylate) (PHMA),<sup>[47]</sup> metallic cores ( $\text{Fe}_3\text{O}_4$ <sup>[48]</sup> and Au<sup>[49]</sup>) polyphosphoester,<sup>[50]</sup> poly(methacryloyloxyethyl phosphorylcholine)<sup>[51]</sup>, hyaluronan,<sup>[52]</sup> sugars (pullulan<sup>[53]</sup> and dextran<sup>[54]</sup>), poly(amino acid)<sup>[55]</sup>. Similar strategies can be used with a range of other drugs.<sup>[56]</sup> In one recent example, Ma and co-workers reported amphiphilic pH-responsive galactosyl dextran-retinal (GDR) nanogels for cancer vaccine delivery, in which all-trans retinal was attached through hydrazone bonds.<sup>[57]</sup>

Hydrazone linkages have also been used to attach releasable PEG layers/shells onto DNA polyplexes.<sup>[58]</sup> The hydrazone conjugated PEG shells act as a releasable shield, which reduces toxicity, prevents aggregation, increases circulation time, and releases via hydrolysis of the hydrazone to expose the positive inner polyplex core. Both *in vitro* and *in vivo* experiments demonstrated significantly higher gene delivery of the polyplexes with hydrazone linkages compared to particles with a stable PEG corona.

Another strategy to incorporate hydrazone linkages into polymer nanoparticles is to introduce a ketone group on the RAFT (reversible addition–fragmentation chain-transfer polymerization) agent, allowing it to be incorporated on the terminal of a controlled radical polymer. Hydrazone bonds can be formed by reacting the end chain of the RAFT polymer with hydrazide functional materials with a variety of biologically useful moieties including fluorophores, MRI contrast agents, and biotin.<sup>[59]</sup>

### 3.2 Imine linkage

Acid labile imine bonds (B, Figure 5) have also been investigated as pH-responsive linkages to design drug loaded nanoparticles.<sup>[60]</sup> In 2014, the Zheng group reported a hydrogen bonding strategy to load hydrophobic drug melphalan into core-shell micelles with carboxymethyl chitosan polymer as the shell.<sup>[60a]</sup> Pyridyl moieties were attached to the polymers via imine linkages and hydrogen bonds were then formed between the pyridine moieties and the drug's amino groups. Selective release of the drug was shown in this system with ~ 65 % release at pH 5.0, whereas release at pH 7.0 and 7.4 was less than 10 %. In 2017, Ding and co-workers reported anticancer nanoparticles based on an imine linked dextran-Dox conjugate (DEX-Dox).<sup>[60b]</sup> In this work, hydroxy groups present on dextran were oxidized to aldehydes, which were then conjugated with Dox via imine formation. This conjugate aggregated into uniform nanoparticles in aqueous solution with an average diameter of ~ 23 nm. DEX-Dox nanoparticles showed slightly better shrinking of a B16F10 tumor than the free Dox control. In addition, the Dox control showed significantly enhanced toxicity in major organs e.g., fracture of muscle fibers in cardiac tissue. In related work, Li et. al. developed a 'nanococktail' for

codelivery of anticancer drugs epirubicin (EPI) and methotrexate (MTX) (Figure 7).<sup>[60c]</sup> MTX is a tumor targeting moiety that was linked to a lipid-PEG conjugate via a covalent imine bond to form the conjugate (DSPE-PEG-CH=N-MTX) while EPI was loaded by complexation with a phospholipid complex (PC). These components were combined via self-assembly to form an MTX targeted nanoparticle. This design allowed the combination of targeting to tumor cells and release of drugs at acidic pH. Flow cytometry analysis showed enhancement in association of MTX targeted particles over the non-targeted particles, this enhancement was removed when the surface was blocked with free folic acid. Despite this evidence of targeting, there was little difference in tumor shrinking when comparing imine and amide stabilized nanoparticles.

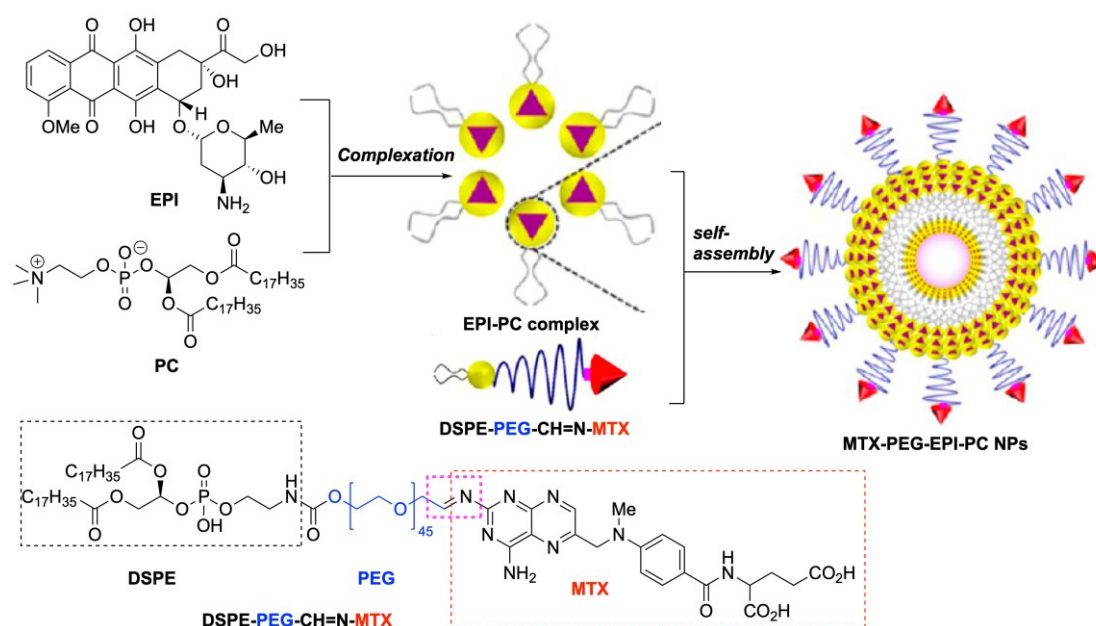


**Figure 7.** Self-assembly of multiple anticancer drugs with pH-responsive imine linkages and lipid-drug complexation. Hydrophilic drug EPI and amphiphilic PC formed the EPI-PC complex via complexation and this complex was then self-assembled with the MTX-PEG-EPI-PC NPs to form the drug-PEG-lipid conjugates (DSPE-PEG-CH=N-MTX). Adapted with permission.<sup>[60c]</sup> Copyright 2017, American Chemical Society.

### 3.3. *cis*-Aconityl (maleic acid amides) linkages

The acid sensitive *cis*-aconityl group (C, Figure 5), in the family of maleic acid amides (MAA), was first used as a pH-responsive linkage for designing PLL/daunomycin polymer-drug conjugates.<sup>[61]</sup> Such linkages have since been applied in a range of polymeric drug carriers using HPMA,<sup>[62]</sup> PAMAM dendrimers,<sup>[63]</sup> PVA (polyvinyl alcohol),<sup>[64]</sup> PLLA-PEG copolymer<sup>[65]</sup>, and oligosaccharides.<sup>[66]</sup>

PAMAM dendrimers have some advantages as carriers for drug delivery such as the ability to induce endosomal escape, however they also exhibit significant non-specificity and cytotoxicity toward normal cells.<sup>[67]</sup> Elsayed and co-workers studied the effects of surface modification of PAMAM dendrimers using PEGylation and sugar or peptide targeting motifs for targeting liver cancer cells.<sup>[63d]</sup> The targeting ligand attached to a linear PEG was grafted on the generation 5 PAMAM dendrimer



**Figure 8.** MAA linkages in siRNA delivery. siRNA is attached to MAA-modified PAsp(DET) via click chemistry and the electrostatic interactions further stabilize the conjugates via formation of polyion complex (PIC) at neutral pH. The siRNA is released under acidic conditions due to degradation of the MMA linkages and formation of the charged PAsp(DET) parent polymer. Adapted with permission.<sup>[71]</sup>

### 3.4. Acetal/ketal linkages

The use of acetals (D, Figure 5) as pH-sensitive linkages for drug delivery was first reported by Fréchet and co-workers in 2004.<sup>[72]</sup> Important work in this area was based on the modification of dextran to form hydrophobic nanoparticles using acetal linkages. These linkages degrade when the pH drops, causing a change in the particle properties from hydrophobic to hydrophilic thus facilitating drug release (Figure 9).<sup>[73]</sup> In their original study, 73% of the hydroxy groups in the dextran polymer were modified with both cyclic and acyclic acetals in the acetalated dextran (Ac-DEX).<sup>[73a]</sup> At 37 °C and physiological pH (7.4), the Ac-DEX had a half-life of 15 days while at mildly acidic pH (5.0) it had a half-life of 10 h. It was also shown these materials had low toxicity.<sup>[1]</sup> The particles were loaded with OVA and showed increased MHC class 1 presentation of the OVA-derived CD8+ T-cell epitope SIINFEKL by a factor of 16 relative to free OVA. A range of drugs including imiquimod<sup>[73d]</sup> plasmid DNA,<sup>[73e]</sup> siRNA,<sup>[73g, 73i]</sup> and antimicrobial agents,<sup>[74]</sup> have also been loaded into the Ac-DEX based particles.

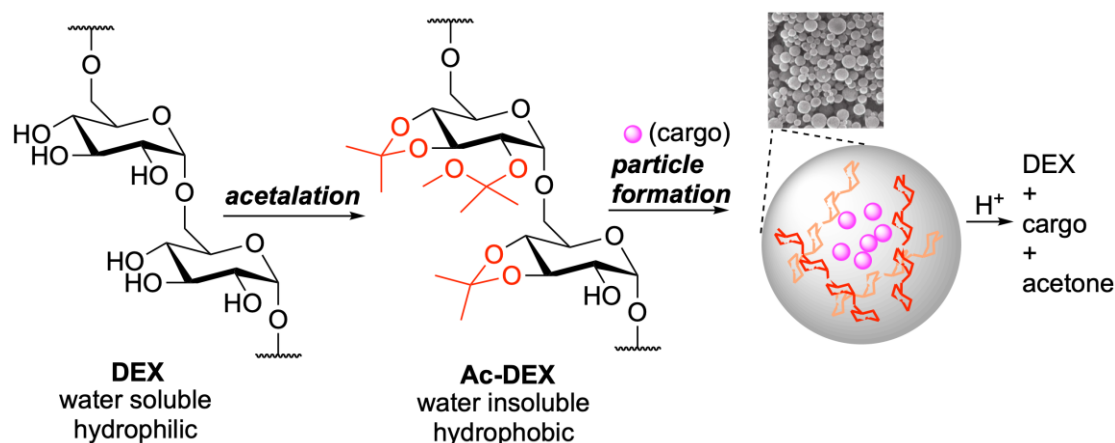


**Figure 9.** Schematic illustration of the acetalation of dextran, nanoparticle formation with drug encapsulation and nanoparticle drug release. Adapted with permission.<sup>[73a]</sup> Copyright 2008, American Chemical Society. Adapted with permission.<sup>[73e]</sup> Copyright 2010, Wiley-VCH.

Almutairi and co-workers varied the acetalation reaction time of dextran to change the ratio of cyclic to acyclic acetals. Using this strategy the degradation rate of the Ac-DEX could be tuned for use in treatment of post-myocardial infarction (MI), which requires drug release over several weeks.<sup>[76]</sup> Other modifications of Ac-DEX have also been reported.<sup>[73h, 77]</sup> The Fréchet group also ligated the Ac-DEX with mannose-based ligands as cell-surface receptors, which were beneficial for antigen delivery.<sup>[73h]</sup> In related work, Boyer and co-workers modified Ac-DEX with macroRAFT agents allowing further modification of Ac-DEX with POEGMA [poly(oligo(ethylene glycol)methyl ether

methacrylate)] copolymer.<sup>[77]</sup> The loading and delivery of anticancer drug Dox with pH-responsive Ac-DEX-POEGMA nanoparticles was investigated.

In more recent work, Meng and co-workers reported micellar nanoparticles comprised of PEG-*b*-PAA copolymers. PAA was functionalized with vinyl ethers and then reacted with paclitaxel (PTX).<sup>[75]</sup> The authors demonstrated the particles could be loaded with up to 43 Wt % PTX. The nanoparticles had similar cell viability to free PTX, with improved killing in the case of PTX resistant cell lines. Notably, a second drug, Dox, could be loaded into the PTX nanoparticles by physical encapsulation and released with change in pH.

### 3.5. *Ortho ester linkages*

*Ortho* esters (E, Figure 5) are a useful type of pH responsive linkage as they are very sensitive to pH and the degraded products are potentially biocompatible. Polymers with *ortho* ester linkages incorporated as pendant groups were first reported by Li and co-workers.<sup>[78]</sup> Wang and co-workers studied the pH-dependant morphological and hydrolytic properties as well as the cytotoxicity of an amphiphilic diblock copolymer, PEG-*b*-PMYM [poly(ethylene glycol)-*b*-poly(*N*-(2-methoxy-[1,3]dioxolan-4-ylmethyl) methacrylamide)] with *ortho* ester pendants.<sup>[79]</sup> They demonstrated that hydrolysis of the *ortho* ester side-chains showed pH-dependant kinetics allowing nanoparticle size to be tuned by pH, e.g., particle size was stable at pH 7.4 but increased at pH 6.0 from ~100 nm to 250 nm over 2 days.

Wang and co-workers have developed DNA delivery systems by synthesizing the polymer PMAOE [poly(*N*-(2-(2-(dimethylamino)ethoxy)-1,3-dioxolan-4-yl)methyl) methacrylamide)] with cationic side-chains linked by *ortho* ester linkages.<sup>[80]</sup> Stable polyplex nanoparticles were formed via electrostatic interactions between the cationic amines and anionic DNA. The release of the cationic functionality using pH responsive linkages is interesting as it offers the advantage of removing the DNA effectively from the polymer backbone. This is challenging for many cationic delivery systems. Slow release of the DNA at pH 4.0 was observed with the hydrolysis of the *ortho* ester (~ 60 % side chain hydrolysis determined using NMR).

### 3.6 *β*-Thiopropionate linkage

The  $\beta$ -thiopropionate group (F, Figure 5), formed by thiol-ene click reactions, have been used as linkages in PEG-siRNA conjugates.<sup>[81]</sup> Recently, the  $\beta$ -thiopropionate linkage was applied by Wooley and co-workers to improve therapeutic efficacy of conjugated drugs.<sup>[82]</sup> The water soluble poly(ethylene oxide)-*b*-polyphosphoester polymer (PEG-*b*-PPE) carrying terminal olefins was prepared via ring opening polymerization (ROP). The thiol-modified PTX was loaded onto the polymer via thiol addition on the olefins, rendering a high drug loading of 53 Wt %. Results showed the *in vitro* cytotoxicity of the nanoparticles against cancer cells was 5-8 times higher than those having non-degradable linkages.

In another study, Hong and co-workers reported a strategy to efficiently load acrylate-conjugated camptothecin (ACPT) by thiol-Michael addition reaction of dihydrolipoic acid pendants with ACPT via formation of  $\beta$ -thiopropionate linkages.<sup>[83]</sup> The release of drugs was shown to be specific as evidenced by 23 % and 50 % of the CPT being released at pH 6.0, after 24 h and 96 h, respectively while no CPT was released at pH 7.4. In addition, better tumor suppression (on ICR mice bearing  $\sim 50 \text{ mm}^3$  subcutaneous tumors) was observed for the prodrug nanoparticles compared to free CPT drug.

### **3.7 pH cleavable moieties within the polymer backbone**

The previous discussion focused on using pH responsive linkages as pendant groups to load drugs or change surface functionality. However, there is also significant work using pH responsive linkages in the polymer backbone. Among these biodegradable linear polymers, poly(*ortho* esters) have the longest history, dating back to the 1970s.<sup>[37a]</sup> The Tang group applied *ortho* ester linkages to improve nanoparticles for gene therapy.<sup>[84]</sup> To reduce the cytotoxicity and increase transfection efficiency of cationic poly(ethylenimine) (PEI) nanoparticles, *ortho* ester linkages were utilized to crosslink the low molecular weight (LMW) PEI. The *in vitro* experiments demonstrated that the pH-responsive polycations (POEIs) had lower cytotoxicity compared to PEI in a number of cell lines and enhanced transfection efficiency in SH-SY5Y cells.

Acetals/ketals linkages have also been used as components in polymeric backbones. Recently, Pu and co-workers reported microspheres based on multiblock poly(L-lactide) (PLLA) with acetal bonds in the backbone.<sup>[85]</sup> The polymer was prepared via two steps, ROP and acetal formation while the drug, Dox was physically loaded into the microsphere particle. One of the challenges with the use of acetal linkages is significant cleavage is commonly observed at pH 7.4, as can be seen in this paper. However, the particles did show an increase in Dox release at pH 5.0 (70%) compared to 7.4 (30%). Another type of poly(acetals) that have been reported are poly(glyoxylates) developed by the Gillies' group.<sup>[86]</sup> These self-immolative polymers degrade by an end-to-end depolymerization mechanism facilitated by cleavage of the end-caps in response to different stimuli, including UV, temperature, oxidants and reductants, either independently or simultaneously. Specifically, when the end-caps are trityl protecting groups, the polymers are pH-responsive.<sup>[86b]</sup>

A variety of acid labile linkages, including hydrazone, imine, acetal, *ortho* ester, maleic acid amide and  $\beta$ -thiopropionate functional groups have been developed and applied in drug delivery. An important consideration when using acid labile linkages is they should have high stability at physiological pH, thus reducing any non-specific release. Hydrazones have been the most commonly studied linkage to date as they are relatively stable at neutral pH while showing good cleavage in mildly acidic environments. Other advantages include easy modification of polymers with necessary functionality and facile formation of the hydrazone linkage. However, with all these chemistries it is often challenging to engineer complete stability at pH 7.4, while retaining efficient cleavage with a decrease of 1 pH unit. Therefore, many studies focus on release at pH 5.0, which means the cargo is

released in the aggressive environment of the lysosome and thus degradation is possible. For this reason, the combination of multiple stimuli is attractive, and we expect this to be the focus of future research.

#### 4. Crosslinking in pH-Responsive Nanoparticles

One challenge with nanoparticle delivery systems is maintaining particle stability, as self assembled materials can change structure when in the biological environment. To enhance the stability of nanoparticles *in vivo*, one strategy is to stabilize them by crosslinking.<sup>[87]</sup> Crosslinking can be through covalent bonds or non-covalent interactions, such as host-guest interaction between  $\beta$ -cyclodextrin ( $\beta$ -CD) and benzimidazole (BM).<sup>[88]</sup> For some applications irreversible crosslinking may be disadvantageous as it can limit the ability to release drug at the target cells. Therefore, it is ideal for crosslinking to be reversible, allowing nanoparticles to break down when the desired site is reached. Disulfide, or pH-sensitive derivatives are some examples of degradable crosslinkers.<sup>[89]</sup> This section will focus on the use of acid labile crosslinking to design better nanoparticle delivery systems.

##### 4.1. pH-cleavable/responsive crosslinkers for the design of nanoparticles

In one interesting study, Zhang and co-workers synthesized core-shell nanogels using free radical polymerization of poly(*N*-isopropylacrylamide) (PNIPAM) in the presence of *N*-lysinal-*N'*-succinyl chitosan (NLSC) with *N*, *N'*-methylene bisacrylamide (MBA) as a crosslinker. The core was then modified by conjugating bovine serum albumin (BSA) as a crosslinked capsid-like shell onto the core. A non-swelling particle was also designed by replacing the *N*-lysinal-*N'*-succinyl chitosan (NLSC) with *N*-lysinal chitosan (NLC). The NLSC particle showed significant swelling, from 200 nm at pH 7.4 to 2  $\mu$ m at pH 4. No swelling was observed for the non-responsive nanoparticles. It was shown that Dox-NLSC particles exhibited bright red fluorescence penetrating ~27 % of a model tumor spheroid, whereas the control particles showed fluorescence only on the outer edge.<sup>[90]</sup>

In a related study, Kang and co-workers used ethylene glycol dimethacrylate (EGDMA) crosslinker to crosslink nanocapsules based on an *in situ* polymerisation of *N*-(3-aminopropyl) methacrylamide (APM) and acrylamide (AAM). The APM was used to bind antisense miR-21 oligonucleotide (AS-miR-21) as a model drug.<sup>[91]</sup> The EGDMA linker could be cleaved by hydrolysis of the ester linkages. pH responsive cleavage was shown by a ~ 60 % decrease in the scattering light intensity when the

particles were incubated at pH 5.4 for 2 h, indicating a decrease in nanoparticles, with no significant change at pH 7.4.<sup>[91]</sup> This formulation inhibited tumor growth for a U87 subcutaneous tumor, growth was two or three-fold slower when treated with the nanoparticles compared to mice treated with either PBS or non-degradable control particles.

In another example, Selvam and co-workers synthesized Ibuprofen-loaded micelles by the reaction of carboxyl-terminated methoxy polyethylene glycol-*b*-polypropylene fumarate (mPEG-PPF) diblock copolymers with Ibuprofen using an anhydride linkage. The fumarate bonds in the PPF backbone were crosslinked with 2-(dimethylamino)ethyl methacrylate by radical polymerization. Drug release was similar for particles containing 10 wt % crosslinker, however, for 17.5 wt % crosslinker there was a considerable difference between drug release at the two pHs, 6.6 and 7.4.<sup>[92]</sup>

Glutaraldehyde can crosslink amine groups by reaction with the aldehyde groups present in its structure. The Schiff base (imine group, C=N) is formed through the nucleophilic attack by the nitrogen of the amino group on the carbon of the glutaraldehyde.<sup>[93]</sup> Importantly, there are some concerns with the use of glutaraldehyde in drug delivery systems as there is inherent toxicity.<sup>[93]</sup> In one recent study, Tang and co-workers used a poly(lysine)-*b*-polycaprolactone (PLL-*b*-PCL) as a self-assembled nanoparticle core. The nanoparticle was crosslinked using glutaraldehyde. Poly (glutamic acid)-*g*-methoxyl poly(ethylene glycol) (PGlu-*g*-mPEG) was then added to form a polyion complex micelle. The PGlu-*g*-mPEG coating was pH dependent and thus was released when the pH decreased. The rate of this charge reversal was tunable based on the crosslinking percentage. It was shown delayed charge reversal had implications in increasing tumor penetration.<sup>[94]</sup>

In another interesting study, Li and co-workers synthesized an amphiphilic polycarbonate, PEG-*b*-P(TMBPEC-*c*-MPMC) [poly(ethylene glycol)-*b*-poly(2,4,6-tri-methoxybenzylidene-pentaerythritol carbonate-*co*-5-methyl-5-propargyl-1,3-dioxan-2-one)] bearing a reactive alkynyl group. Crosslinking was achieved using azide-alkyne click chemistry by the addition of 1,6-diazidohexane and bis(azido-ethyl)disulfide to form pH-sensitive crosslinked micelles (CCL/CC) and combined pH and redox responsive crosslinked micelles (CCL/SS) respectively. For CCL/CC micelles, at pH 7.4, Dox release was ~32 % over 48 h, whereas it was ~ 61 % at pH 5. This increase in drug release was believed to be due to hydrolysis of acetal groups resulting in an increase in hydrophilicity of the hydrophobic core under acidic conditions. It was also shown that Dox loaded CCL/SS micelles had greater cytotoxicity in drug resistant cells compared to CCL/CC (which are only pH responsive) and they were both significantly more potent than free Dox.<sup>[95]</sup>

In another study using ketal based crosslinkers, Lee and co-workers designed self-assembled poly(ethylene glycol)-*b*-(L-aspartic acid)-*b*-(L-phenylalanine) (PEG-*b*-PAsp-*b*-PPhe) micelles with PEG forming the outer corona, PAsp as the middle shell, and PPhe as the inner core. To stabilize the nanoparticle structure, the Asp functional groups were reacted with diamine crosslinker containing a ketal linkage. The half-life of ketal hydrolysis was found to be 52 h at pH 7.4 whereas it was only 0.7 h at pH 5.0 (74-fold faster hydrolysis).<sup>[96]</sup> pH responsive crosslinked nanoparticles have also been used for the delivery of cisplatin. Stenzel and co-workers used crosslinked micelles based on triblock copolymers of poly(oligo(ethylene glycol) methyl-ether methacrylate)-*b*-poly(*N*-hydroxysuccinic methacrylate)-*b*-poly(1,1-di-*tert*-butyl 3-(2-(methacryloyloxy)ethyl) butane-1,1,3-tricarboxylate) (POEGMEMA-*b*-PNHSMA-*b*-PMAETC).<sup>[97]</sup> A ketal diamino crosslinker were reacted with the activated ester units within the copolymer at the interface between core and shell. The cis-dichlorodiamino platinum (II) was complexed to the polymer through the deprotected malonic acid groups. An IC<sub>50</sub> of 16.7 μM was reported for carboplatin. Higher cytotoxicity was observed for crosslinked micelles (IC<sub>50</sub>, 35 μM, three times lower at 24 h) than un-crosslinked micelles (90 μM) for OVCAR-3 cells.<sup>[97]</sup> Interestingly, while the IC<sub>50</sub> of acid cleavable particles (35 μM) was lower than the non-cleavable linkers (80 μM) at 24 h, this difference was reduced at 72 h (5.0 μM and 6.0 μM, respectively).

In a recent study, Haag and co-workers used polyglycerol as a building block for nanoparticles that could be tuned from 100 nm to 1000 nm. Dendritic polyglycerol nanogels were synthesized by reaction of polyglycerol modified with *p*-propargyloxy benzacetale with polyglycerol modified with azide functionality using click chemistry (Figure 10). The diameter of the particles had a direct correlation with the concentration of macromolecules in the aqueous phase during the nanoprecipitation process. The final particle sizes were tunable (in a range of 100 to 1000 nm) with low polydispersity and high retention of cargo. Interestingly, release of protein (asparaginase) from these particles was highly specific, with almost no release at pH 7.4, and complete release at pH 5.<sup>[98]</sup>

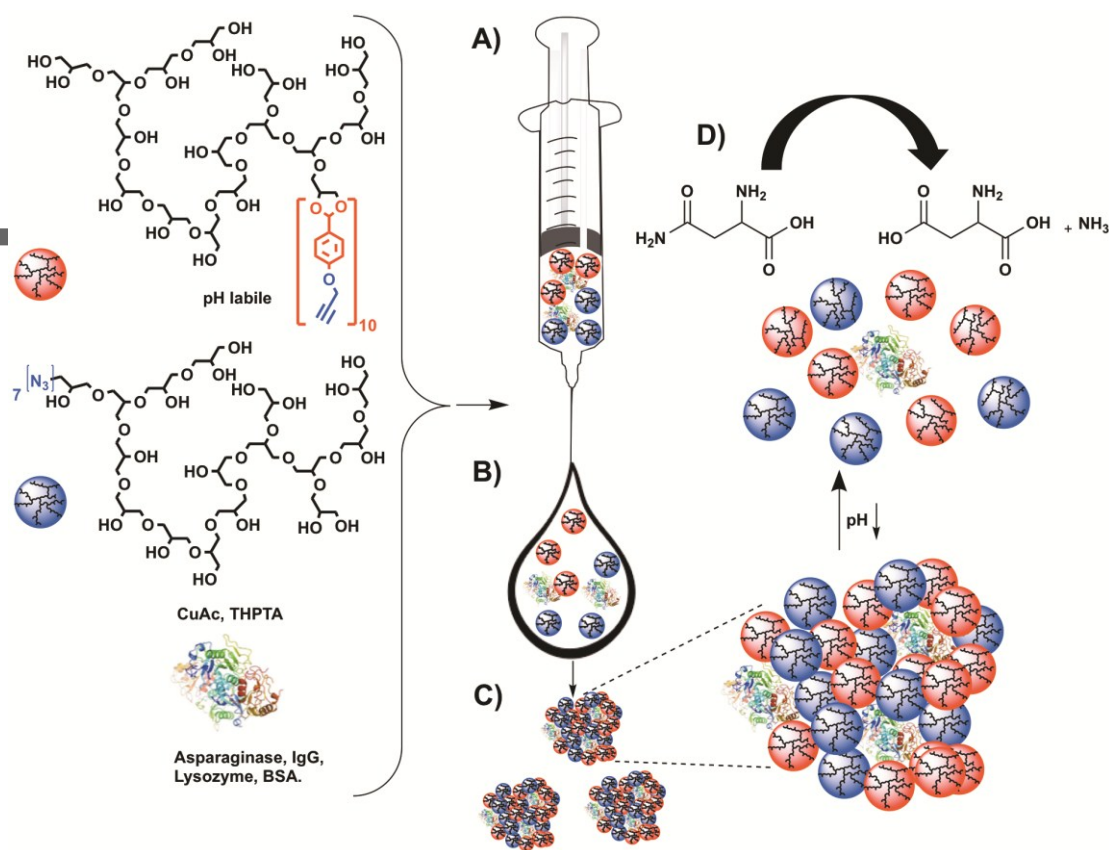


**Figure 10.** Preparation of polyglycerol nanogels by nanoprecipitation. A) The particles were synthesized by injection of an aqueous solution of alkyne-functionalized polyglycerol macromonomers (red spheres), azide-functionalized polyglycerol macromonomers (blue spheres) and the protein cargo, asparaginase, IgG, Lysozyme or BSA. B) The particle was formed by diffusion of the aqueous phase into the acetone phase. C) The particles were crosslinked by azide and alkyne 2+3 cycloaddition, and finally, D) degradation-triggered release of asparagine and its catalytic conversion of asparagine to aspartic acid under ammonia generation was investigated.<sup>[98]</sup>

In a study to investigate multidrug resistance, Tang and co-workers prepared pH-sensitive nanogels (NG1) and P-glycoprotein-repressive nanogels (NG2) by copolymerization between an ortho ester-based crosslinker, *N,N'*-(((4,4'-(oxybis(methylene))bis(1,3-dioxolane-4,2-diy))bis(oxy))bis(ethane-2,1-diy))bis(2-methylacrylamide) (OEAM) and methacrylate modified dextran. NG2 particles were also modified with tocopheryl polyethylene glycol succinate (TPGS).<sup>[99]</sup> These particles were loaded with Dox and their ability to bypass multi drug resistance was examined. The cytotoxicity of the particles (both NG1 and NG2) in MCF-7 cells was similar to free Dox, however in the drug resistant cell line MCF-7/ADR the IC<sub>50</sub> was ~106 µg/mL for free Dox whereas it was ~10 µg/mL for NG2 (lower than that of NG1, ~110 µg/mL). Interestingly, it was ~12 µg/mL for TPGS + Dox suggesting some of this enhancement was not due to the nanoparticle but instead due to the use of TPGS.<sup>[99]</sup>

#### 4.1.1. Host-guest recognition

In host-guest interactions, two or more molecules or ions are held together with non-covalent bonds, such as hydrogen bonds, ionic bonds, van der Waals forces, and hydrophobic interactions.

Cyclodextrins are well known to facilitate host-guest interactions. They are a class of cyclic oligosaccharides and consist of six, seven, or eight glucose units linked by  $\alpha$ -1,4- linkages which are called  $\alpha$ -,  $\beta$ -, and  $\gamma$ -cyclodextrin respectively. Cyclodextrins are able to encapsulate hydrophobic drugs because of their hydrophobic cavity (inside the oligosaccharide rings), forming a host-guest complex.<sup>[100]</sup> Recently, these materials have been applied to the design of pH responsive nanoparticles. Deng and co-workers synthesized particles based on the combination of two polymers, poly((methacrylic acid betaine) methyl methacrylate)-*b*-poly(single 6-methyl acryloyl ethylenediamine  $\beta$ -cyclodextrin)-*b*-poly(benzimidazole ethyl methacrylate)-*b*-poly(diisopropylamino ethyl methacrylate) (PCB-*b*-PCD-*b*-PDPAEMA) and poly((methacrylic acid betaine) methyl methacrylate)-*b*-poly(benzimidazole ethyl methacrylate)-*b*-poly(diisopropylamino ethyl methacrylate) (PCB-*b*-PBM-*b*-PDPAEMA).<sup>[88]</sup> To form crosslinked particles, both polymers were employed while non-crosslinked particles involved just a single polymer (PCB-*b*-PCD-*b*-PDEAEMA). The pH-responsive PDPAEMA ( $pK_a \approx 6.3$ ) acted as the core, hydrophilic PCB acted as the shell and the pH-responsive host-guest complex was based on  $\beta$ -CD and BM ( $pK_a < 6.0$ ). Nanoparticles were made through solvent evaporation method and crosslinked based on host-guest recognition between  $\beta$ -CD ( $\beta$ -cyclodextrin) and BM (benzimidazole).<sup>[88]</sup> Below pH 6.0, the amino groups of BM ( $pK_a < 6.0$ ) are protonated which makes the host-guest complexes unstable and thus the particles disassembled.<sup>[88]</sup> The crosslinked particle showed significantly enhanced stability to dilution with unimodal peaks being maintained even at 1000-fold dilution, whereas non-crosslinked particle became unstable under these conditions. Interestingly, there was limited difference in their cell viability when loaded with Dox.

#### 4.1.2. Metal ions

Metal-phenolic networks are interesting as a self-assembling material because they are versatile and their cytotoxicity is negligible.<sup>[101]</sup> Recently, Caruso and co-workers applied oleic acid (OA) to make emulsions via ultrasonic emulsification, which led to the formation of droplets smaller than 200 nm in diameter (Figure 11).<sup>[101]</sup> These OA/water emulsions were employed as templates for interfacial self-assembly of metal-phenolic networks (MPNs). To coat the emulsion, the authors used 8 arm PEG-polyphenol and  $\text{Fe}^{\text{III}}\text{Cl}_3 \cdot 6\text{H}_2\text{O}$  in 3-(*N*-morpholino)propanesulfonic acid (MOPS) buffer. MPNs were formed on the surface of the emulsion phase by self-assembly of the PEG polyphenols and  $\text{Fe}^{\text{III}}$ . The resulting nanoparticles were shown to release Dox specifically at pH 5.0 and have a circulation half-life of ~50 min *in vivo*.<sup>[101]</sup>

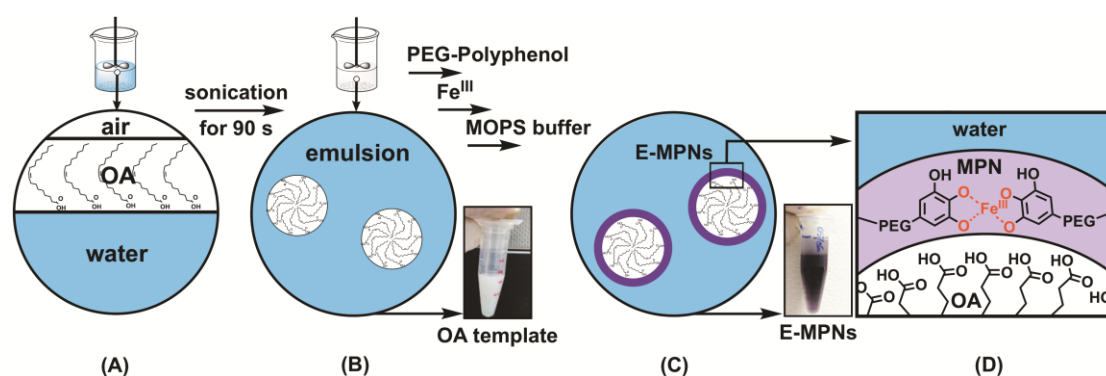


**Figure 11.** Schematic of the deposition of PEG-polyphenol MPNs on oleic acid (OA) emulsions (E-MPNs). A) Sonication of OA mixture in water and B) adding PEG-polyphenol to the OA emulsion. After incubating PEG-polyphenol for 20 min,  $\text{Fe}^{\text{III}}\text{Cl}_3 \cdot 6\text{H}_2\text{O}$  was added and then the pH was raised to 8 with 3-(*N*-morpholino)propanesulfonic acid (MOPS) buffer resulting in a purple dispersion. C) The digital photograph indicates the purple color of resultant (0.3% OA/ $\text{H}_2\text{O}$  (v/v)) compared to its color in the last step (B). D) The successful chelation of  $\text{Fe}^{\text{III}}$  by phenolic moieties on PEG-polyphenol to form a polymeric film. Adapted with permission.<sup>[101]</sup>

#### 4.2. Particles with a combination of multiple stimuli responsive moieties

The combination of multiple stimuli-responsive moieties within the same nanoparticle has received significant interest for improving the specificity of therapeutic release. In one recent study, Liu and co-workers synthesized shell crosslinked micelles with amphiphilic poly( $\epsilon$ -caprolactone)-*b*-poly((oligo(ethylene glycol) monomethyl ether methacrylate-*co*-*p*-(methacryloxyethoxy)benzaldehyde)) (PCL-*b*-P(OEGMA-*co*-MAEBA)) diblock copolymers. Shell crosslinked nanoparticles were synthesized by crosslinking aldehyde groups using dithiolbis(propanoic dihydrazide), thus making the particle responsive to both pH and redox variation.<sup>[102]</sup> Camptothecin (CPT) was loaded into crosslinked (SCL) and non-crosslinked (NCL) particles and the release investigated. Lower non-specific release was seen for the dual responsive SCL particles (~18% at pH 7.4), compared to ~56% release from NCLs at pH 7.4. A drop in pH from 7.4

to 5.0 or adding DTT (10 mM) made release faster, however, using both stimuli simultaneously was more effective, making drug release close to that for non-crosslinked micelles.<sup>[102]</sup>

In another study, Shuai and co-workers synthesized crosslinked micelles based on a triblock copolymer of monomethoxy polyethylene glycol (mPEG), 2-mercaptoethylamine (MEA)-grafted poly(L-aspartic acid) (PAsp(MEA)), and 2-(diisopropylamino)ethyl-amine (DIP)-grafted poly(L-aspartic acid) (PAsp(DIP)) (Figure 12). Particles were formed at pH 10, followed by disulfide crosslinking of the MEA groups and then adjusting pH to 7.4. The particles were also loaded with Dox. At pH 7.4 the particles were ~60 nm in diameter, however they swelled to ~300 nm at pH 5.0, and ~550 nm at pH 7.4 with DTT. In the absence of DTT, no Dox release was observed at pH 7.4, whereas approximately 40 % release occurred at pH 5.0 after 10 h. Significant Dox release was observed after 5 h (95%) in the presence of 10 mM DTT.<sup>[103]</sup> This polymer was also used in later work (Dai and co-workers) to form pH/redox responsive gold nanocages. The nanoparticles had no detected Dox release after 24 h at pH 7.4, however, nanoparticles released drug at pH 5.0 with 10 mM GSH after 5 h (approximately 40% of Dox).<sup>[104]</sup>

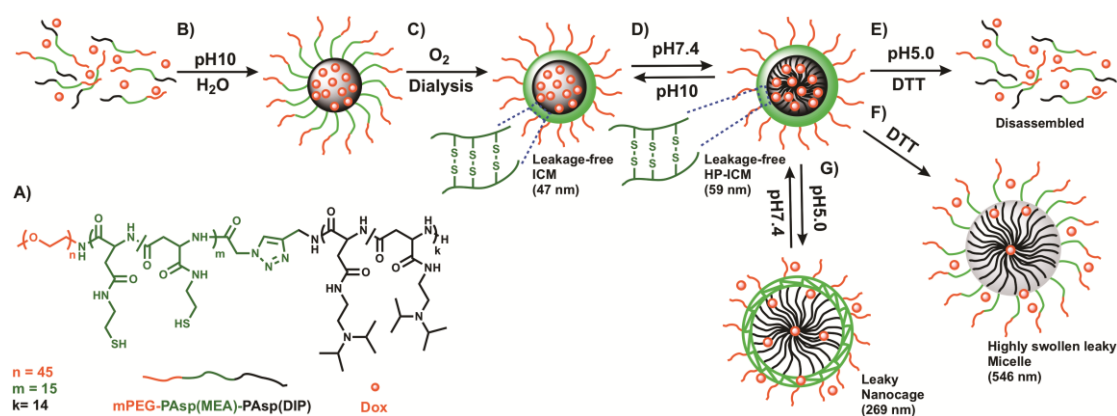


**Figure 12.** Formation and structural transitions of the dual-sensitive, highly packed interlayer-crosslinked micelle (HP-ICM) ( $n$ ,  $m$  and  $k$  represent the degree of polymerization for three different blocks which are  $n = 45$ ,  $m = 15$ ,  $k = 14$ ). A) The structure of the mPEG-*b*-PAsp(MEA)-*b*-PAsp(DIP) copolymer. B) Self-assembly of mPEG-*b*-PAsp(MEA)-*b*-PAsp(DIP) copolymers at pH 10, C) Interlayer crosslinking upon disulfide formation with the MEA groups which creates a tight layer (green) around the core and a small micelle size because of complete deprotonation of DIP groups at pH 10. D) Adjusting the pH of the solution to pH 7.4, resulting in an expansion due to partial protonation of DIP groups. E) Disassembly of particles at pH 5.0 in combination with DTT. F) Increase in leakiness with the addition of 10 mM DTT due to the removal of the crosslinking stabilization. G) Complete protonation of DIP groups at pH 5.0, leading to the significant swelling and thus enhanced drug release.<sup>[103]</sup>

In another example, Zhong and co-workers used poly(ethylene glycol)-*b*-poly(mono-2,4,6-trimethoxy benzylidene-pentaerythritol carbonate-*co*-pyridyl disulfide carbonate) [PEG-*b*-P(TMBPEC-*co*-PDSC)] block copolymers to form Dox-loaded micelles with a core containing pH-tunable TMBPEC and pyridyl disulfide groups allowing formation of redox responsive crosslinks. Dox release from the

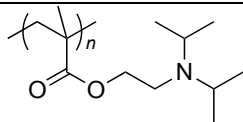
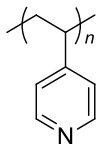
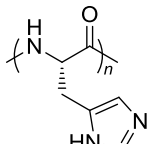
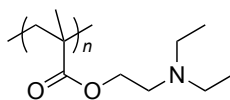
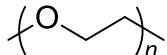
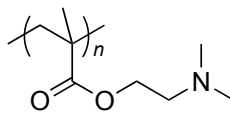
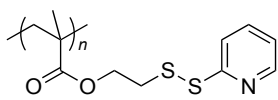
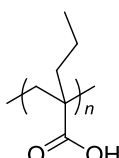
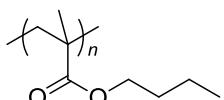
particles was limited at 7.4 (~ 20%) but increased when the pH dropped to pH 5.0, or in the presence of 10 mM GSH at pH 7.4 (~64 % and ~44 % respectively). Importantly, drug release with the combination of pH 5.0 and 10 mM GSH was almost complete (~99 %).<sup>[105]</sup> The crosslinked particles had low IC<sub>50</sub> values for HeLa and RAW 264.7 cells of 1.65 µg DOX equivalent/mL and 1.14 µg Dox equivalent/mL as compared to Dox control of 0.41 µg/mL and 0.38 µg/mL.

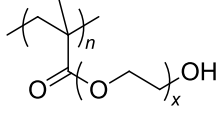
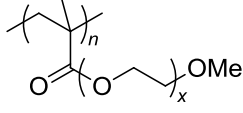
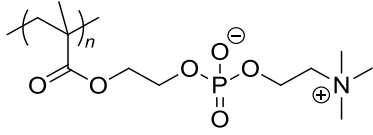
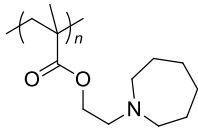
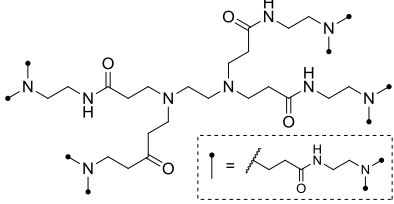
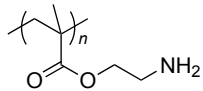
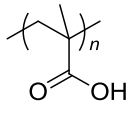
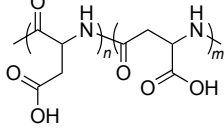
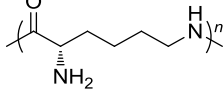
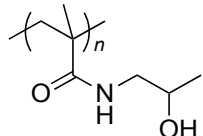
In similar work, Dong and co-workers self-assembled a triblock copolymer, polycarboxybetaine methacrylate-*b*-poly(*N*-(2-(2-pyridyl disulfide) ethyl methacrylamide-*b*-poly(2-(diisopropylamino) ethyl methacrylate) (PCB-*b*-PDSEMA-*b*-PDPAEMA) and crosslinked via disulfide crosslinking. The surface of the particles was modified with Arg-Gly-Asp (RGD) to increase cell binding.<sup>[106]</sup> It was shown the release rates from the particles could be controlled by crosslinking density.<sup>[106]</sup> Release rates were higher at low pH (pH 5.0) or with addition of 10 mM GSH. However, the most efficient release was seen with a combination of stimuli giving 100 % Dox release after 5 h. Interestingly, there was only small differences in the cytotoxicity of these particles compared to a non-crosslinked control. In another system, Li and co-workers incorporated pH and redox responsive components based on poly[oligo (ethylene glycol) fumarate-*co*-dithiodiethanol fumarate] (POEGSSFM) micelles, with Dox-SH conjugated to the fumarate block. These particles were in situ core-crosslinked with 1,6-hexanedithiol through a Michael addition thiol-ene “click” reaction. Results showed specific release of Dox with the combination of pH 5.8 and 10 mM GSH (~70%), with limited release at pH 7.4 with and without DTT (~5%).<sup>[107]</sup> It has been demonstrated in a related study (Kwon and co-workers) that crosslinking can control release rate of cargo.<sup>[108]</sup> pH and redox responsive moieties have also been used to design particles with a charge shifting shell and a responsive crosslinked core (Park and co-workers).<sup>[109]</sup>

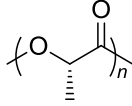
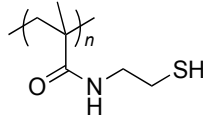
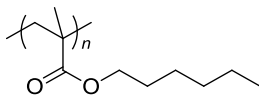
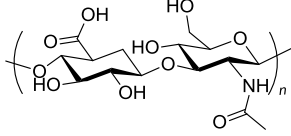
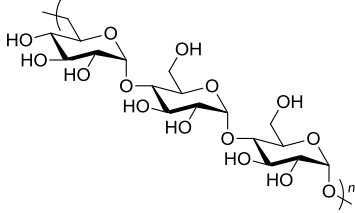
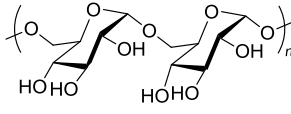
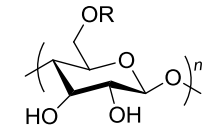
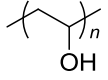
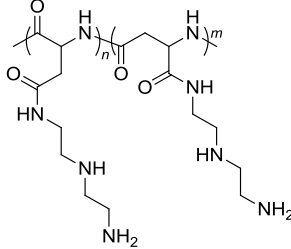
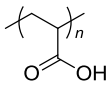
A number of studies have shown the advantages of crosslinking to enhance the stability of nanoparticles before they reach their target site. However, nanoparticle cleavage that relies on degradation of covalent bonds can be slow, especially if there are only small differences between the cleavage environment and physiological pH. Thus, non-covalent strategies are of interest, such as the complexation of iron and polyphenol. In addition, strategies to combine different crosslinking

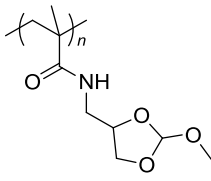
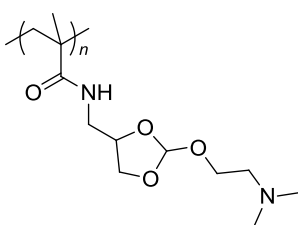
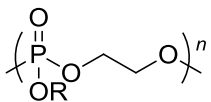
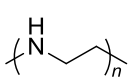
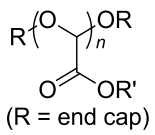
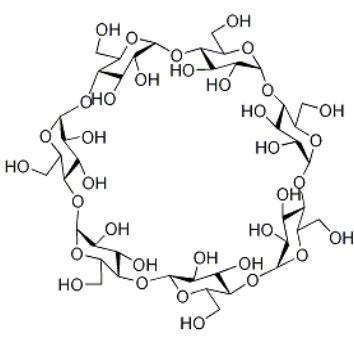
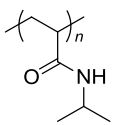
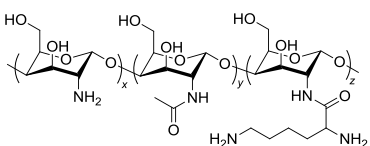
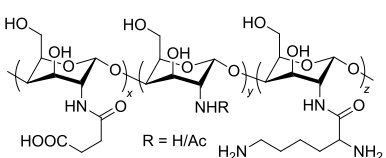
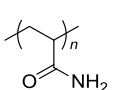
moieties have potential to enhance specificity of drug release and are an exciting direction of future research.

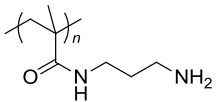
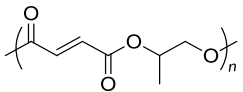
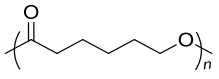
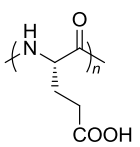
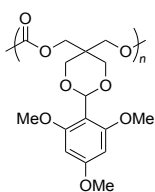
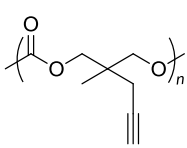
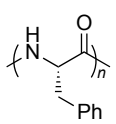
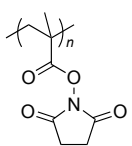
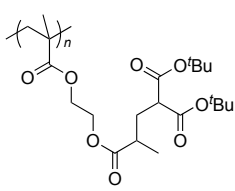
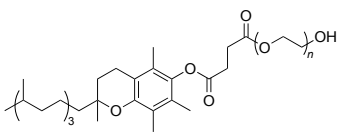
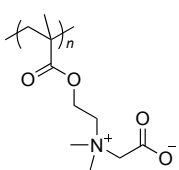
**Table 1.** Polymer structures discussed within this review.

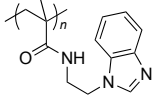
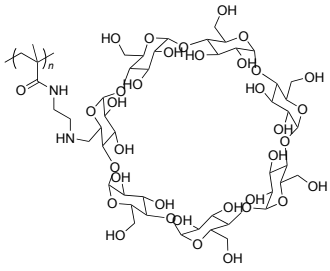
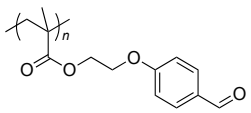
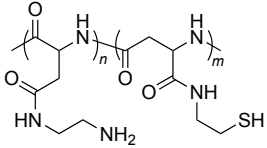
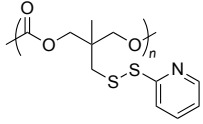
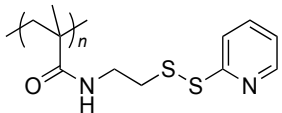
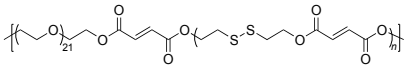
Acronym	Name	Structure	Ref.
PDPAEMA	Poly(2-(diisopropylamino)ethyl methacrylate)		7b, 8a, 17, 18, 21, 88, 104, 106
P4VP	Poly(4-vinyl pyridine)		8b
-	Poly(histidine)		8c, 9a
PDEAEMA	Poly(2-diethylamino)ethyl methacrylate		10, 15, 27
PEG	Poly(ethylene glycol)		
PDMAEMA	Poly(2-(dimethylamino)ethyl methacrylate)		12, 17
Poly(PDSEMA)	Poly(pyridyl disulfide ethyl methacrylate)		12
PPAA	Poly(propyl acrylic acid)		12, 34, 36a
PBMA	Poly(butyl methacrylate)		12, 15

PPEGMA	Poly(poly(ethylene glycol) methacrylate)		15
PEO	Poly(ethylene oxide)	$\text{H}(\text{OCH}_2\text{CH}_2)_n\text{OH}$	16
POEGMA	Poly(oligo(ethylene glycol)methyl ether methacrylate)		18, 97
PMPC	Poly(2-(methacryloyloxy)ethyl phosphorylcholine)		18, 51
P123	Poly(ethylene glycol)- <i>b</i> -poly(propylene glycol)- <i>b</i> -poly(ethylene glycol)	$\text{H}(\text{OCH}_2\text{CH}_2)_x(\text{OCH}_2\text{CH}_2\text{CH}_2)_y(\text{OCH}_2\text{CH}_2)_z\text{OH}$	24
PAEMA	Poly(2-azepane ethyl methacrylate)		25
PAMAM	Poly(amidoamine)		25, 45, 63
PAEMA	Poly(2-aminoethyl methacrylate)		27
PMAA	Poly(methacrylic acid)		28, 29, 30, 42
PAsp	Poly(aspartic acid)		30, 71a, 96
PLL	Poly(L-lysine)		34
PHPMA	Poly( <i>N</i> -(2-hydroxypropyl) Methacrylamide))		39, 62

PLLA (PLA)	Poly(L-lactide)		41, 65, 85
PMA <sub>SH</sub>	–		42
PHMA	Poly(hexyl methacrylate)		47
–	Hyaluronan or Hyaluronic acid		52, 70
–	Pullulan		53
DEX	Dextran		54, 60b, 72, 73, 76, 77
–	Chitosan	 R = chitosan R = CH <sub>2</sub> COOH, carboxymethyl chitosan	60a, 90
PVA	Polyvinyl alcohol		64
PAsp(DET)	–		71a
PAA	Poly(acrylic acid)		75

PMYM	Poly(ethylene glycol)- <i>b</i> -poly( <i>N</i> -(2-methoxy-[1,3]dioxolan-4-ylmethyl) methacrylamide)		79
PMAOE	Poly( <i>N</i> -((2-(2-(dimethylamino)ethoxy)-1,3-dioxolan-4-yl)methyl) methacrylamide)		80
PPE	Polyphosphoester		82
PEI	Poly(ethylene imine)		84
–	Poly(glyoxylate)		86
β-CD	β-cyclodextrin		88
PNIPAM	Poly( <i>N</i> -isopropylacrylamide)		90
NLC	<i>N</i> -lysinal chitosan		90
NLSC	<i>N</i> -lysinal- <i>N'</i> -succinyl chitosan		90
PAAM	Poly(acrylamide)		91

PAPM	Poly( <i>N</i> -(3-aminopropyl) methacrylamide)		91
PPF	Poly(propylene fumarate)		92
PCI	Poly(caprolactone)		94, 102
PGlu	Poly(glutamic acid)		94
PTMBPEC	Poly(2,4,6-tri-methoxybenzylidene-pentaerythritol carbonate)		95, 105
PMPMC	Poly(5-methyl-5-propargyl-1,3-dioxan-2-one)		95
PPhe	Poly(L-phenylalanine)		96
PNHSMA	Poly( <i>N</i> -hydroxysuccinic methacrylate)		97
PMAETC	Poly(1,1-di- <i>tert</i> -butyl 3-(2-(methacryloyloxy) ethyl) butane-1,1,3-tricarboxylate)		97
TPGS	Tocopheryl poly(ethylene glycol succinate)		99
PCB	Poly((methacrylic acid betaine) methyl methacrylate)		88

PBM	Poly(benzimidazole ethyl methacrylate)		88
PCD	Poly(single 6-methyl acryloyl ethylenediamine $\beta$ -cyclodextrin)		88
PMAEBA	Poly( <i>p</i> -(methacryloxyethoxy)benzaldehyde)		102
PAsp(MEA)	2-mercaptoethylamine-grafted poly(L-aspartic acid)		104
PPDSC	Poly(pyridyl disulfide carbonate)		105
PDS	Poly( <i>N</i> -(2-(2-pyridyl disulfide) ethyl methacrylamide)		106
POEGSSFM	Poly(oligo(ethylene glycol) fumarate-co-dithiodiethanol fumarate)		107

## 5. Conclusion

A number of elegant strategies have been employed to design pH responsive nanoparticles for therapeutic delivery. These particles can be engineered with pH degradable linkages, pH cleavable crosslinking or incorporating charge shifting polymers. These strategies enable the particles to deliver their therapeutic specifically in response to pH changes found in the acidic compartments within the cell (endosomes, lysosomes) or in acidic tumor tissue. Some of these materials have also demonstrated the potential to deliver cargo to the cytosol, overcoming a significant limitation with many nanoparticle delivery systems, where the therapeutic cargo is trapped and degraded in the lysosomes. However, there are still challenges remaining before these materials are translated to the clinic. Issues such as biodistribution and the non-specific accumulation of nanoparticles in organs such as the liver, still limit the *in vivo* use of many nanoparticles. In addition, there is still a lot to be learnt about targeting nanoparticles to specific regions. Many targeted systems show limited benefit over their non-targeted variants in an *in vivo* setting. Furthermore, while some materials presented in this review show some degree of endosomal escape, the efficiency of escape generally remains low and thus further work is required to significantly improve the efficiency. It is also challenging to compare different delivery systems across studies as there is wide variation in cell or tumor types and experimental protocols used. Nanomedicine would benefit from the development of standardized assays which could be used to benchmark new particles developed against existing materials. In summary, it is vital that new delivery systems are combined with greater understanding of the nanoparticle/biological interactions so we can build a guidebook for better material design.

**Acknowledgements:** The authors would like to thank the Australian Research Council (DP180100844) and the National Health and Medical Research Council (APP1129672) for funding.

**Keywords:** pH responsive nanoparticles, drug delivery, stimuli-responsive, charge shifting, pH cleavable

## References

- [1] D. Bobo, K. J. Robinson, J. Islam, K.J. Thurecht, *Pharm.Res.* **2016**, *33*, 2373.
- [2] R. Cheng, F. Meng, C. Deng, H. A. Klok, Z. Zhong, *Biomaterials* **2013**, *34*, 3647.
- [3] M. Wei, Y. Gao, X. Li, M. J. Serpe, *Polym. Chem.* **2017**, *8*, 127.
- [4] M. Karimi, A. Ghasemi, P. S. Zangabad, R. Rahighi, S. M. Moosavi, B. H. Mirshekari, M. Amiri, Z. S. Pishabad, A. Aslani, M. Bozorgomi, D. Ghosh, A. Bezvavi, A. Vaseghi, A. R. Aref, L. Haghani, S. Bahrami, M. R. Hamblin, *Chem. Soc. Rev.* **2016**, *45*, 1457.
- [5] G. K. Such, Y. Yan, A. P. Johnston, S. T. Gunawan, F. Caruso, *Adv. Mater.* **2015**, *27*, 2278
- [6] L. I. Selby, C. M. C. Jugo, G. K. Such, A. P. R. Johnston, *Wires. Nanomed. Nanobi.* **2016**, *9*,1452.
- [7] a) A. S. M. Wong, S. K. Mann, E. Czuba, A, Sahut, H. Liu, T. C. Suekama, T. Bickerton, A. P. R. Johnston, G. K. Such, *Soft Mater.* **2015**, *11*, 2993 ; b) H. L. Chang, S. K. Kang, J. A. Lim, H. S. Lim, J. H. Cho, *Soft Mater.* **2012**, *8*, 10238.
- [8] a) S. T. Gunawan, K. Liang, G. K. Such, A. P. R. Johnson, M. K. M. Leung, J. Cui, F. Caruso, *Small* **2014**, *10*, 4080 ; b) W. Zhang, L. Shi, R. Ma, Y. An, Y. Xu, K. Wu, *Macromolecules* **2005**, *38*, 8850 ; c) P. Bilalis, L. Tziveleka, S. Varlas, H. Latrous, *Polym. Chem*, **2016**,*7*, 1475.
- [9] a) H. Wu, L. Zhu, V. P. Torchilin, *Biomaterials* **2013**, *194*, 1213; b) K. Liang, J. Richardson, H. Ejima, G. K. Such, F. Caruso, *Adv. Mater.* **2014**, *15*, 2398.
- [10] A. S. M. Wong, S. K. Mann, E. Czuba, A, Sahut, H. Liu, T. C. Suekama, T. Bickerton, A. P. R. Johnston, G. K. Such, *Soft Mater.* **2015**, *15*, 2993.
- [11] N. Kongkatigumjorn, S. A. Smith, M. Chen, K. Fang, SH. Yang, E. R. Gillies, A. P. R. Johnston, G, Such, *ACS Appl. Nano Mater.* **2018**, *1*, 3164.
- [12] J. T. Wilson, S. Keller, M. J. Manganiello, C. Cheng, C. C. Lee, C. Opara, A. Convertine, P. S. Stayton, *ACS Nano* **2013**, *7*, 3912.
- [13] S. Keller, J. T. Wilson, G. I. Patilea, H. B. Kern, A. J. Convertine, P. S. Stayton, *J. Controlled Release* **2014**. *191*, 214.
- [14] J. T. Wilson, A. Postma, S. Keller, A. J. Convertine, G. Moad, E. Rizzardo, L. Meagher, J. Chiefari, P. S. Stayton, *AAPS J.* **2015**, *17*, 358.
- [15] H. B. Kern, S. Srinivasan, A. J. Convertine, D. Hockenbery, O. W. Press, P. S. Stayton, *Mol. Pharmaceutics* **2017**, *14*, 1450.

- [16] K. Zhou, Y. Wang, X. Huang, K. L. Phelps, B. D. Sumer, J. Gao, *Angew. Chem., Int. Ed. Engl.* **2011**, *236*, 6109.
- [17] H. Yu, Y. Zou, Y. Wang, X. Huang, G. Huang, B. D. Sumer, D. A. Boothman, J. Gao, *ACS Nano* **2011**, *11*, 9246.
- [18] E. Ellis, K. Zhang, Q. Lin, E. Ye, A. Poma, G. Battaglia, X. J. Loh, T. Ch. Lee, *J. Mater. Chem. B*, **2017**, *5*, 4421.
- [19] Z. Wang, M. Luo, Ch. Mao, Q. wei, T. Zhao, Y. Li, G. Huang, J. Gao, *Angew. Chem. Int. Ed. Engl.* **2017**, *56*, 1319.
- [20] M. Luo, H. Wang, Z. Wang, H. Cai, Z. Lu, Y. Li, M. Du, G. Huang, Ch. Wang, X. Chen, M. R. Porembka, J. Lee, A. E. Frankel, Y. X. Fu, Z. J. Chen, J. Gao, *Nat. Nanotechnol.* **2017**, *12*, 648.
- [21] H. Yu, C. Guo, J. Liu, X. Chen, D. Wang, L. Teng, Y. Li, Q. Yin, Z. Zhang, Y. Li, *Theranostics* **2016**, *6*, 14.
- [22] H. Yu, Y. Zou, L. Jiang, Q. Yin, X. He, L. Chen, Z. Zhang, W. Gu, Y. Li, *Biomaterials* **2013**, *34*, 2738.
- [23] H. Yu, Z. Xu, X. Chen, L. Xu, Q. Yi, Z. Zhang, Y. Li, *Macromol. Biosci.* **2014**, *14*, 100.
- [24] H. Yu, Z. Cui, P. Yu, Ch. Guo, B. Feng, T. Jiang, S. Wang, Q. Yin, D. Zhong, X. Yang, Z. Zhang, Y. Li, *Adv. Funct. Mater.* **2015**, *25*, 2489.
- [25] H. J. Li, J. Zh. Du, J. Liu, X. J. Du, S. Shen, Y. H. Zhu, X. Wang, X. Ye, Sh. Nie, J. Wang, *ACS Nano* **2016**, *10*, 6753.
- [26] S. Lee, X. Tong, F. Yang, *Biomater. Sci.* **2016**, *4*, 405.
- [27] Y. Hu, T. Litwin, A. R. Nagaraja, B. Kwong, J. Katz, N. Watson, D. J. Irvine, *Nano Letters* **2007**, *7*, 3056.
- [28] Y. L. Luo, W. Yu, F. Xu, *Polym. Bull.* **2012**, *69*, 597
- [29] M. Abbasian, M. M. Roudi, F. Mahmoodzadeh, M. Eskandani, M. Jaymand, *Int. J. Biol. Macromol.* **2018**, *11*, 1871
- [30] Y. Zhao, H. J. Su, L. Fang and T. W. Tan, *Polymer* **2005**, *46*, 5368.

- [31] B. A. Abel, M. B. Sims, Ch. L. McCormick, *Macromolecules* **2015**, *48*, 5487.
- [32] P. D. Pickett, Ch. R. Kasprzak, D. T. Siefker, B. A. Abel, M. A. Dearborn, C. L. McCormick, *Macromolecules* **2018**, *51*, 9052.
- [33] K. Han, J. Zhang, W. Zhang, Sh. Wang, L. Xu, C. Zhang, X. Zhang, H. Han, *ACS Nano* **2017**, *11*, 3178.
- [34] H. C. Kang, H. Bae, *Adv. Funct. Mater.* **2007**, *17*, 1263.
- [35] M. A. Yessine, M. Lafleur, C. Meier, H. U. Petereit, J. Ch. Leroux, *Biochim. Biophys. Acta* **2003**, *101*, 28.
- [36] T. R. Kyriakides, C.Y. Cheung, N. Murthy, P. Bornstein, P. S. Stayton, A. S. Hoffman, *J. Controlled Release* **2002**, *47*, 295; b) A. J. Convertine, D. S. W. Benoit, C. L. Duvall, A. S. Hoffman, P. S. Stayton, *J. Controlled Release* **2009**, *349*, 229.
- [37] a) S. Binauld, M. H. Stenzel, *Chem. Commun.* **2013**, *49*, 2082; b) X. Pang, Y. Jiang, Q. Xiao, A. W. Leung, H. Hua, C. Xu, *J. Controlled Release* **2016**, *222*, 116; c) Y. Kakizawa, K. Kataoka, *Adv. Drug Delivery Rev.* **2002**, *54*, 203; d) D. R. Vogus, V. Krishnan, S. Mitragotri, *Curr. Opin. Colloid Interface Sci.* **2017**, *31*, 75.
- [38] W. R. Algar, D. E. Prasuhn, M. H. Stewart, T. L. Jennings, J. B. Blanco-Canosa, P. E. Dawson, I. L. Medintz, *Bioconjugate Chem.* **2011**, *22*, 825.
- [39] a) J. Kopeček, P. Kopecková, T. Minko, Z. Lu, *Eur. J. Pharm. Biopharm.* **2000**, *50*, 61; b) P. Chytil, E. Koziolova, T. Etrych, K. Ulbrich, *Macromol. Biosci.* **2018**, *18*, 1700209.
- [40] T. Etrych, M. Jelínková, B. Říhová, K. Ulbrich, *J. Controlled Release* **2001**, *73*, 89.
- [41] S. Aryal, C.-M. J. Hu, L. Zhang, *ACS Nano* **2010**, *4*, 251.
- [42] J. Cui, Y. Yan, Y. Wang, F. Caruso, *Adv. Funct. Mater.* **2012**, *22*, 4718.
- [43] C. Fang, F. M. Kievit, Y.-C. Cho, H. Mok, O. W. Press, M. Zhang, *Nanoscale* **2012**, *4*, 7012.
- [44] Y. Zhao, Z. H. Houston, J. D. Simpson, L. Chen, N. L. Fletcher, A. V. Fuchs, I. Blakey, K. J. Thurecht, *Mol. Pharmaceutics* **2017**, *14*, 3539.
- [45] K. Kono, C. Kojima, N. Hayashi, E. Nishisaka, K. Kiura, S. Watarai, A. Harada, *Biomaterials* **2008**, *29*, 1664.
- [46] W. She, K. Luo, C. Zhang, G. Wang, Y. Geng, L. Li, B. He, Z. Gu, *Biomaterials* **2013**, *34*, 1613.

- [47] a) P. Chytil, T. Etrych, C. Konak, M. Sirova, T. Mrkvan, J. Boucek, B. Rihova, K. Ulbrich, *J. Controlled Release* **2008**, *127*, 121; b) S. K. Filippov, P. Chytil, P. V. Konarev, M. DyakonOVA, C. Papadakis, A. Zhigunov, J. Plestil, P. Stepanek, T. Etrych, K. Ulbrich, D. I. Svergun, *BioMacromolecules* **2012**, *13*, 2594; c) S. K. Filippov, J. M. Franklin, P. V. Konarev, P. Chytil, T. Etrych, A. Bogomolova, M. Dyakonova, C. M. Papadakis, A. Radulescu, K. Ulbrich, P. Stepanek, D. I. Svergun, *BioMacromolecules* **2013**, *14*, 4061; d) X. Zhang, B. J. Niebuur, P. Chytil, T. Etrych, S. K. Filippov, A. Kikhney, D. C. F. Wieland, D. I. Svergun, C. M. Papadakis, *Biomacromolecules* **2018**, *19*, 470.
- [48] a) Q. Yuan, R. Venkatasubramanian, S. Hein, R. D. K. Misra, *Acta Biomater.* **2008**, *4*, 1024; b) J. Zhang, R. D. K. Misra, *Acta Biomater.* **2007**, *3*, 838.
- [49] M. S. Hudlikar, X. R. Li, I. A. Gagarinov, N. Kolishetti, M. A. Wolfert, G. J. Boons, *Chem. Eur. J.* **2016**, *22*, 1415.
- [50] C.-Y. Sun, S. Dou, J.-Z. Du, X. Z. Yang, Y.-P. Li, J. Wang, *Adv. Healthcare Mater.* **2014**, *3*, 261.
- [51] X. Chen, S. S. Parelkar, E. Henchey, S. Schneider, T. Emrick, *Bioconjugate Chem.* **2012**, *23*, 1753.
- [52] M. Xu, J. Qian, A. Suo, H. Wang, X. Yong, X. Liu, R. Liu, *Carbohydr. Polym.* **2013**, *98*, 181.
- [53] a) D. Lu, X. Wen, J. Liang, Z. Gu, X. Zhang, Y. Fan, *J. Biomed. Mater. Res. B.* **2009**, *89b*, 177; b) H. Wang, G. Wan, Y. Liu, B. Chen, H. Chen, S. Zhang, D. Wang, Q. Xiong, N. Zhang, Y. Wang, *Polym. Chem.* **2016**, *7*, 6340.
- [54] Y. Zhang, H. Wang, J. F. Mukerabigwi, M. Liu, S. Luo, S. Lei, Y. Cao, X. Huang, H. He, *RSC Adv.* **2015**, *5*, 71164.
- [55] B. Li, M. Shan, X. Di, C. Gong, L. Zhang, Y. Wang, G. Wu, *RSC Adv.* **2017**, *7*, 30242.
- [56] a) S. Li, L. Wang, N. Li, Y. C. Liu, H. Su, *Biomed. Pharmacother.* **2017**, *95*, 548; b) O. Sedlacek, M. Hruby, M. Studenovsky, D. Vetvicka, J. Svoboda, D. Kankova, J. Kovar, K. Ulbrich, *Bioorg. Med. Chem.* **2012**, *20*, 4056; c) H. Li, M. Li, C. Chen, A. Fan, D. Kong, Z. Wang, Y. Zhao, *Int. J. Pharm.* **2015**, *495*, 572.
- [57] C. Wang, P. Li, L. Liu, H. Pan, H. Li, L. Cai, Y. Ma, *Biomaterials* **2016**, *79*, 88.
- [58] G. F. Walker, C. Fella, J. Pelisek, J. Fahrmeir, S. Boeckle, M. Ogris, E. Wagner, *Mol. Ther.* **2005**, *11*, 418.
- [59] S. Bandyopadhyay, X. Xia, A. Maiseiyeu, G. Mihai, S. Rajagopalan, D. Bong, *Macromolecules* **2012**, *45*, 6766.
- [60] a) W. Wang, H. Yang, X. Kong, Z. Ye, Y. Yin, X. Zhang, G. He, P. Xu, H. Zheng, *RSC Adv.* **2014**, *4*, 28499; b) X. Feng, D. Li, J. Han, X. Zhuang, J. Ding, *Mater. Sci. Eng. C.* **2017**, *76*, 1121; c) Y. Li, L. Song, J. Lin, J. Ma, Z. Pan, Y. Zhang, G. Su, S. Ye, F.-H. Luo, X. Zhu, Z. Hou, *ACS Appl. Mater. Interfaces* **2017**, *9*, 39127.
- [61] W.-C. Shen, H. J. P. Ryser, *Biochem. Biophys. Res. Commun.* **1981**, *102*, 1048.

- [62] a) W.-M. Choi, P. Kopečková, T. Minko, J. Kopeček, *J. Bioact. Compat. Polym.* **1999**, *14*, 447; b) P. Chytil, T. Etrych, C. Konak, M. Sirova, T. Mrkvan, B. Rihova, K. Ulbrich, *J. Controlled Release* **2006**, *115*, 26.
- [63] a) S. Zhu, M. Hong, G. Tang, L. Qian, J. Lin, Y. Jiang, Y. Pei, *Biomaterials* **2010**, *31*, 1360; b) S. Zhu, M. Hong, L. Zhang, G. Tang, Y. Jiang, Y. Pei, *Pharm. Res.* **2010**, *27*, 161; c) L. Zhang, S. Zhu, L. Qian, Y. Pei, Y. Qiu, Y. Jiang, *Eur. J. Pharm. Biopharm.* **2011**, *79*, 232; d) S. H. Medina, G. Tiruchinapally, M. V. Chevliakov, Y. Y. Durmaz, R. N. Stender, W. D. Ensminger, D. S. Shewach, M. E. Elsayed, *Adv. Healthcare Mater.* **2013**, *2*, 1337; e) K. Wang, X. Zhang, Y. Liu, C. Liu, B. Jiang, Y. Jiang, *Biomaterials* **2014**, *35*, 8735; f) J. Nie, Y. Wang, W. Wang, *Int. J. Pharm.* **2016**, *509*, 168; g) J. Zhu, G. Wang, C. S. Alves, H. Tomas, Z. Xiong, M. Shen, J. Rodrigues, X. Shi, *Langmuir* **2018**, *34*, 12428.
- [64] A. Kakinoki, Y. Kaneo, Y. Ikeda, T. Tanaka, K. Fujita, *Biol. Pharm. Bull.* **2008**, *31*, 103.
- [65] H. S. Yoo, E. A. Lee, T. G. Park, *J. Controlled Release* **2002**, *82*, 17.
- [66] F. -Q. Hu, L. -N. Liu, Y. -Z. Du, H. Yuan, *Biomaterials* **2009**, *30*, 6955.
- [67] K. Jain, P. Kesharwani, U. Gupta, N. K. Jain, *Int. J. Pharm.* **2010**, *394*, 122.
- [68] H. Song, J. Zhang, W. Wang, P. Huang, Y. Zhang, J. Liu, C. Li, D. Kong, *Colloids Surf., B* **2015**, *136*, 365.
- [69] T. Suma, J. Cui, M. Müllner, Y. Ju, J. Guo, M. Hu, F. Caruso, *ACS Macro Lett.* **2015**, *4*, 160.
- [70] C. -J. Lin, C. -H. Kuan, L. -W. Wang, H. -C. Wu, Y. Chen, C. -W. Chang, R. -Y. Huang, T. -W. Wang, *Biomaterials* **2016**, *90*, 12.
- [71] a) H. Takemoto, K. Miyata, S. Hattori, T. Ishii, T. Suma, S. Uchida, N. Nishiyama, K. Kataoka, *Angew. Chem. Int. Ed.* **2013**, *52*, 6218; b) F. Pittella, H. Cabral, Y. Maeda, P. Mi, S. Watanabe, H. Takemoto, H. J. Kim, N. Nishiyama, K. Miyata, K. Kataoka, *J. Controlled Release* **2014**, *178*, 18; c) M. Tangsangasakri, H. Takemoto, M. Naito, Y. Maeda, D. Sueyoshi, H. J. Kim, Y. Miura, J. Ahn, R. Azuma, N. Nishiyama, K. Miyata, K. Kataoka, *Biomacromolecules* **2016**, *17*, 246.
- [72] E. R. Gillies, A. P. Goodwin, J. M. Fréchet, *Bioconjugate Chem.* **2004**, *15*, 1254.
- [73] a) E. M. Bachelder, T. T. Beaudette, K. E. Broaders, J. Dashe, J. M. Fréchet, *J. Am. Chem. Soc.* **2008**, *130*, 10494; b) K. E. Broaders, J. A. Cohen, T. T. Beaudette, E. M. Bachelder, J. M. Fréchet, *Proc. Natl. Acad. Sci. U.S.A.* **2009**, *106*, 5497; c) J. A. Cohen, K. E. Broaders, T. T. Beaudette, E. M. Bachelder, J. M. J. Fréchet, *J. Immunol.* **2009**, *182*; d) E. M. Bachelder, T. T. Beaudette, K. E. Broaders, J. M. Fréchet, M. T. Albrecht, A. J. Mateczun, K. M. Ainslie, J. T. Pesce, A. M. Keane-Myers, *Mol. Pharmaceutics* **2010**, *7*, 826; e) J. A. Cohen, T. T. Beaudette, J. L. Cohen, K. E. Broaders, E. M. Bachelder, J. M. Fréchet, *Adv. Mater.* **2010**, *22*, 3593; f) J. A. Cohen, T. T. Beaudette, J. L. Cohen, K. E. Broaders, E. M. Bachelder, J. M. J. Fréchet, *Adv. Mater.* **2010**, *22*, 3593; g) J. L. Cohen, S. Schubert, P. R. Wich, L. Cui, J. A. Cohen, J. L. Mynar, J. M. Fréchet, *Bioconjugate Chem.* **2011**, *22*, 1056; h) L. Cui, J. A. Cohen, K. E. Broaders, T. T. Beaudette, J. M. J. Fréchet, *Bioconjugate Chem.* **2011**, *22*, 949; i) L. Cui, J. L. Cohen, C. K. Chu, P. R. Wich, P. H. Kierstead, J. M. J. Fréchet, *J. Am. Chem. Soc.* **2012**, *134*, 15840.

- [74] C. Ornelas-Megiatto, P. N. Shah, P. R. Wich, J. L. Cohen, J. A. Tagaev, J. A. Smolen, B. D. Wright, M. J. Panzner, W. J. Youngs, J. M. Fréchet, C. L. Cannon, *Mol. Pharmaceutics* **2012**, *9*, 3012
- [75] Y. Gu, Y. Zhong, F. Meng, R. Cheng, C. Deng, Z. Zhong, *Biomacromolecules* **2013**, *14*, 2772.
- [76] a) S. Suarez, G. N. Grover, R. L. Braden, K. L. Christman, A. Almutairi, *Biomacromolecules* **2013**, *14*, 3927; b) S. L. Suarez, A. Munoz, A. C. Mitchell, R. L. Braden, C. Luo, J. R. Cochran, A. Almutairi, K. L. Christman, *ACS Biomater. Sci. Eng.* **2016**, *2*, 197.
- [77] H. T. T. Duong, F. Hughes, S. Sagnella, M. Kavallaris, A. Macmillan, R. Whan, J. Hook, T. P. Davis, C. Boyer, *Mol. Pharmaceutics* **2012**, *9*, 3046.
- [78] a) X. Huang, F. Du, J. Cheng, Y. Dong, D. Liang, S. Ji, S.-S. Lin, Z. Li, *Macromolecules* **2009**, *42*, 783; b) X. Huang, F. Du, R. Ju, Z. Li, *Macromol. Rapid Commun.* **2007**, *28*, 597; c) X. Huang, F. Du, D. Liang, S.-S. Lin, Z. Li, *Macromolecules* **2008**, *41*, 5433.
- [79] R. Tang, W. Ji, C. Wang, *Macromol. Biosci.* **2010**, *10*, 192.
- [80] Z. Xu, J. Lai, R. Tang, W. Ji, R. Wang, J. Wang, C. Wang, *Macromol. Biosci.* **2014**, *14*, 1015.
- [81] M. Oishi, Y. Nagasaki, K. Itaka, N. Nishiyama, K. Kataoka, *J. Am. Chem. Soc.* **2005**, *127*, 1624.
- [82] J. Zou, F. Zhang, S. Zhang, S. F. Pollack, M. Elsabahy, J. Fan, K. L. Wooley, *Adv. Healthcare Mater.* **2014**, *3*, 441.
- [83] C.-R. Xu, L. Qiu, C.-Y. Pan, C.-Y. Hong, Z.-Y. Hao, *Bioconjugate Chem.* **2018**, *29*, 3203.
- [84] L. Zhang, M. Yu, J. Wang, R. Tang, G. Yan, W. Yao, X. Wang, *Macromol. Biosci.* **2016**, *16*, 1175.
- [85] J. Li, X. Zhang, M. Zhao, L. Wu, K. Luo, Y. Pu, B. He, *Biomacromolecules* **2018**, *19*, 3140.
- [86] a) B. Fan, J. F. Trant, A. D. Wong, E. R. Gillies, *J. Am. Chem. Soc.* **2014**, *136*, 10116; b) B. Fan, J. F. Trant, E. R. Gillies, *Macromolecules* **2016**, *49*, 9309; c) B. Fan, J. F. Trant, R. E. Yardley, A. J. Pickering, F. Lagagne-Labarthe, E. R. Gillies, *Macromolecules* **2016**, *49*, 7196; d) B. Fan, E. R. Gillies, *Mol. Pharmaceutics* **2017**, *14*, 2548; e) B. Fan, R. Salazar, E. R. Gillies, *Macromol. Rapid Commun.* **2018**, *39*; f) B. Fan, R. E. Yardley, J. F. Trant, A. Borecki, E. R. Gillies, *Polym. Chem.* **2018**, *9*, 2601; g) A. Rabiee Kenaree, E. R. Gillies, *Macromolecules* **2018**, *51*, 5501.
- [87] a) M. Li, Z. Tang, S. Lv, W. Song, H. Hong, X. Jing, Y. Zhang, X. Chen, *Biomaterials* **2014**, *35*, 3851; b) Y. Yang, Y. Li, Q. Lin, C. Bao, L. Zhu, *ACS Macro Lett.* **2016**, *5*, 301; c) H. Cabral, K. Miyata, K. Osada, K. Kataoka, *Chem. Soc. Rev.* **2018**, *118*, 6844.
- [88] H. Feng, Y. Sun, J. Zhang, L. Deng, A. Dong, *J. Drug Delivery Sci. Technol.* **2018**, *45*, 81.
- [89] H. S. Han, T. Thambi, K. Y. Choi, S. Son, H. Ko, M. C. Lee, D.-G. Jo, Y. S. Chae, Y. M. Kang, J. Y. Lee, J. H. Park, *BioMacromolecules* **2015**, *16*, 447.
- [90] C. Ju, R. Mo, J. Xue, L. Zhang, Z. Zhao, L. Xue, Q. Ping, C. Zhang, *Angew. Chem. Int. Ed.* **2014**, *53*, 6253.

- [91] C. Liu, J. Wen, Y. Meng, K. Zhang, J. Zhu, Y. Ren, X. Qian, X. Yuan, Y. Lu, C. Kang, *Adv. Mater.* **2015**, *27*, 292.
- [92] G. Seetharaman, A. R. Kallar, V. M. Vijayan, J. Muthu, S. Selvam, *J Colloid Interface Sci.* **2017**, *492*, 61.
- [93] B. Sarmiento, J. das Neves, *Chitosan-Based Systems for Biopharmaceuticals*, **2012**.
- [94] J. Gou, Y. Liang, L. Miao, W. Guo, Y. Chao, H. He, Y. Zhang, J. Yang, C. Wu, T. Yin, Y. Wang, X. Tang, *Acta Biomater.* **2017**, *62*, 157.
- [95] X.-Q. Yi, Q. Zhang, D. Zhao, J.-Q. Xu, Z.-L. Zhong, R.-X. Zhuo, F. Li, *Polym. Chem.* **2016**, *7*, 1719.
- [96] S. J. Lee, K. H. Min, H. J. Lee, A. N. Koo, H. P. Rim, B. J. Jeon, S. Y. Jeong, J. S. Heo, S. C. Lee, *BioMacromolecules* **2011**, *12*, 1224.
- [97] V. T. Huynh, S. Binauld, P. L. de Souza, M. H. Stenzel, *Chem. Mater.* **2012**, *24*, 3197.
- [98] D. Steinhilber, M. Witting, X. Zhang, M. Staegemann, F. Paulus, W. Friess, S. Kuchler, R. Haag, *J. Controlled Release* **2013**, *169*, 289.
- [99] M. Sun, X. Wang, X. Cheng, L. He, G. Yan, R. Tang, *Carbohydr. Polym.* **2018**, *198*, 142.
- [100] a) N. Sharma, A. Baldi, *Drug Delivery* **2014**, *23*, 739; b) S. Datz, B. Illes, D. Gößl, C. v. Schirnding, H. Engelke, T. Bein, *Nanoscale* **2018**, *10*.



**Nayeleh Deirram** is currently a PhD student at the University of Melbourne under the supervision of Dr. Georgina Such and Dr. Angus Johnston. She graduated with a Master of Polymer Science from the University of Technology Malaysia (UTM) in 2012. Her PhD studies focus on the use of pH responsive nanoparticles for probing cellular delivery.



**Angus P.R. Johnston** is the head of the NanoMaterials for Biology Lab at the Monash Institute of Pharmaceutical Sciences. His group focuses on understanding the interactions between nanomaterials and cells to enable the development of more efficient drug delivery systems. His research interests include intracellular trafficking, protein engineering, targeted nanoparticle delivery, quantitative molecular sensors, advanced fluorescence imaging, and nanoparticle engineering.

**Georgina Such** completed her PhD in 2006 from the University of New South Wales, Australia. She is currently a senior lecturer in the School of Chemistry, running a research team focused on the design and application of functional materials. Her research interests include self-assembly, stimuli-responsive nanoparticles and studying nanoparticle/biological interactions.



**pH-Responsive nanoparticles** have significant potential for improving the efficiency of therapeutic delivery. This review discusses the three main strategies to design such materials, including the use of charge-shifting polymers, acid-labile side-chains, and pH-responsive crosslinking. Recent examples of pH-responsive nanoparticles are also highlighted.

Drug Delivery

pH-Responsive Polymer Nanoparticles for Drug Delivery

N. Deirram, C. Zhang, S. S. Kermanian, A. P. R. Johnston, Georgina K. Such\*

